AD-A124 609 THE LAST 14 DAYS OF SKYLAB 1: ORBIT DETERMINATION AND ANALYSIS(U) ROYAL AIRCRAFT ESTABLISHMENT FARNBOROUGH (ENGLAND) D M WALKER JUN 82 RAE-TR-82067 DRIC-TR-82-67 1/1

UNCLASSIFIED F/G 22/3 NL

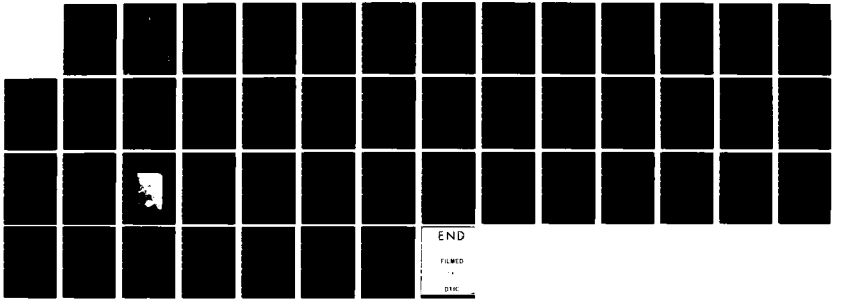

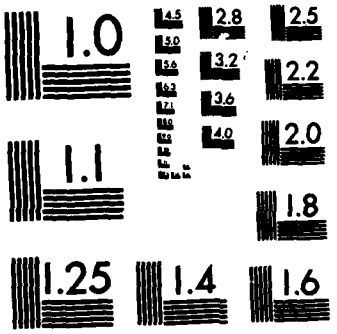

TR 82067

REPRINT

ROYAL AIRCRAFT ESTABLISHMENT

*

. Technical Report 82067

June 1982

THE LAST 14 DAYS OF SKYLAB 1: ORBIT DETERMINATION AND ANALYSIS

by

Doreen M. C. Walker

*

Procurement Executive, Ministry of Defence
Farnborough, Hants

UNLIMITED

UDC 629.195 : 5.006.2 : 521.3 : 629.19.077.3

ROYAL AIRCRAFT ESTABLISHMENT

Technical Report 82067

Received for printing 18 June 1982

THE LAST 14 DAYS OF SKYLAB 1: ORBIT DETERMINATION AND ANALYSIS

by

Doreen M. C. Walker

SUMMARY

The orbit of Skylab 1 (1973-27A) has been determined using some 1400 NORAD observations during the 14 days prior to decay on 1979 July 11. There are 14 daily orbits, with standard deviations corresponding to average accuracies of 40 m cross track and 30 m radial. A 15th orbit, only slightly less accurate, was determined from observations on July 11 between the manoeuvre at 07.45 UT and decay at 16.37 UT.

The variations in inclination due to atmospheric rotation and 16th-order resonance with the geopotential have been successfully analysed, to give the first values of 16th-order geopotential coefficients determined from resonance, and a value of 1.10 ± 0.07 rev/day for the atmospheric rotation rate at a height of 210-220 km.

The daily changes in semi-major axis have been used to determine 13 daily values of air density, at heights from 252 km down to 179 km. All agree well with the *CIRA 1972* model, and indicate a smaller semi-annual variation than in the early 1970s.

The variations of eccentricity and argument of perigee take unusual forms, but detailed analysis shows that the variations are in full accord with the theory for an atmosphere with day-to-night variation in density, with the perigee progressing towards the point of minimum density.

Departmental Reference: Space 617

UNLIMITED

LIST OF CONTENTS

1 INTRODUCTION

Skylab 1, 1973-27A, was launched on 14 May 1973 at 17.30 UT into a nearly circular orbit inclined at 50° to the equator[1]. The central structure of the spacecraft was cylindrical[2], 25.6 m long and 6.6 m in diameter, while its solar panels gave it an overall span of 27.4 m (see Fig 1), and its mass was 74783 kg.

Three separate crews manned Skylab between 23 May 1973 and 8 February 1974, and after this date the spacecraft was left to decay naturally. The total lifetime for Skylab was then predicted by RAE as 6 years[3]. This prediction proved to be very good, well within the usual error for lifetime predictions, 10% of the remaining lifetime. An account of subsequent prediction by RAE is given in Ref 4. Skylab finally decayed on 11 July 1979 at 16.37 UT over SW Australia in the full glare of press publicity, after 2249 days in orbit.

After the decay, over 2000 observations of the satellite, made during its last 15 days in orbit by the assigned and contributing sensors of the North American Air Defense Command (NORAD), Space Detection and Tracking System (SPADATS), were made available to us, and in this Report the observations have been analysed to give daily orbits using the RAE orbit refinement program PROP in the PROP 6 version[5].

2 THE ORBITS

2.1 Up to July 9

In the PROP 6 model the mean anomaly M is [illegible]ed by a polynomial of the form

$$M = M_0 + M_1 t + M_2 t^2 + M_3 t^3 + M_4 t^4 + M_5 t^5 \quad , \qquad (1)$$

where t is the time measured from epoch, and the number of M coefficients used depends on the severity and variability of the drag. The orbital elements for the first 13 orbits determined daily from June 27 to July 9 are given in Table 1, with the standard deviations below each value. The epoch for each orbit is at 00 h on the day indicated.

As the individual orbits were determined from observations extending over less than 24 hours, so that $t < 0.5$, it would be expected that only a small number of coefficients in equation (1) would be required. This proved to be true, with seven orbits needing only $M_0 - M_2$ and the remaining six $M_0 - M_3$. The orbit determined on June 27, using only 25 observations poorly distributed around the orbit, was not reliable, the value of inclination in particular being badly in error. So in the subsequent analysis this orbit (given in square brackets in Table 1) was ignored, the orbit for June 28 being regarded as orbit 1. The orbit for June 27 is included in Table 1 to illustrate the bias errors that can occur when the distribution of observations is poor.

Table 1

Values of the orbital parameters, with standard deviations, for orbits 1 to 12

	MJD	Date 1979	a	e	i	Ω	ω	ω + M_0	M_1	M_2	M_3	ε	N	D	a - 6372
	[44051.0	June 27	6627.403	0.000991	50.0217	56.431	104.1	230.528	5792.314	1.658	-	0.30	25	0.86	255.40]
			6	26	38	1	8		8	26					
1	44052.0	June 28	6624.924	0.000907	50.0280	50.830	101.7	269.108	5795.565	1.643	-	0.34	99	0.92	252.92
			1	5	3	<1	3		1	5					
2	44053.0	June 29	6622.465	0.000833	50.0277	45.227	102.4	310.927	5798.793	1.635	-	0.36	91	0.95	250.47
			1	4	3	<1	3		1	5					
3	44054.0	June 30	6619.818	0.000757	50.0253	39.612	105.9	356.047	5802.272	1.892	-	0.31	92	0.99	247.82
			1	3	4	<1	3		1	4					
4	44055.0	July 1	6616.741	0.000690	50.0245	33.989	108.2	44.938	5806.318	2.033	-0.26	0.24	47	0.86	244.74
			4	5	4	1	5		5	12	3				
5	44056.0	July 2	6613.448	0.000580	50.0240	28.355	106.0	98.018	5810.656	2.255	-	0.30	64	0.99	241.45
			1	5	4	1	6		1	6					
6	44057.0	July 3	6609.932	0.000500	50.0234	22.713	107.4	155.623	5815.292	2.414	0.09	0.35	87	0.93	237.93
			3	4	3	1	6		4	4	2				
7	44058.0	July 4	6605.904	0.000421	50.0238	17.062	105.5	218.136	5820.611	2.959	0.21	0.35	90	0.93	233.90
			3	4	2	<1	6		4	4	2				
8	44059.0	July 5	6601.114	0.000329	50.0226	11.395	96.8	286.551	5826.946	3.340	0.29	0.37	79	0.87	229.11
			3	5	2	<1	7		4	4	2				
9	44060.0	July 6	6595.690	0.000231	50.0220	5.715	88.8	1.708	5834.134	3.718	-	0.33	67	0.87	223.69
			1	4	2	<1	1.1		1	4					
10	44061.0	July 7	6589.564	0.000197	50.0188	0.015	74.8	84.470	5842.272	4.533	0.39	0.34	85	1.00	217.56
			2	4	4	1	1.6		3	4	2				
11	44062.0	July 8	6581.786	0.000166	50.0169	354.293	53.0	176.447	5852.629	5.564	-	0.40	77	0.92	209.79
			1	6	4	1	1.9		1	5					
12	44063.0	July 9	6572.544	0.000142	50.0161	348.545	12.6	279.703	5864.975	7.040	0.47	0.33	87	0.87	200.54
			2	4	4	1	1.4		3	8	2				

Key: MJD = modified Julian day

a = semi major axis (km)

e = eccentricity

i = inclination (deg)

Ω = right ascension of ascending node (deg)

ω = argument of perigee (deg)

M_0 = mean anomaly at epoch (deg)

M_1 = mean motion n (deg/day)

M_2, M_3 = later coefficients in the polynomial for M

ε = measure of fit

N = number of observations used

D = time covered by the observations (days)

For the 12 daily orbits from June 28 to July 9 (orbits 1 to 12), the observations for each orbit are much more numerous and are fitted in a satisfactory manner, with ε, the parameter indicating the measure of fit, always between 0.24 and 0.40. It would appear that the range error allocated to the NORAD observations could be reduced, because the range residual is very small for the great majority of observations. For these 12 orbits the average standard deviation in inclination is 0.0003°, equivalent to 35 m in cross-track distance, and 0.000004 in eccentricity, equivalent to 30 m in radial distance.

The last column in Table 1 gives the mean height of the satellite, 6372 km being the appropriate mean Earth radius.

2.2 For July 10.0

During its last 2 days in orbit Skylab was tracked by nearly every available radar because it was known that quite large sections would survive re-entry and fall somewhere on the Earth's surface. The idea was to obtain observations and keep updating the impact prediction, and if it seemed that Skylab's last orbit would be over a highly populated area, attitude changes would be made. In consequence, many hundreds of observations were available; about 600 from midday on July 9 to midday on July 10, and about 800 between midday on July 10 and decay at 16.37 UT on July 11.

The 600 observations centred on July 10.0 fell into two groups of about 300, one before and one after midnight. At first, as PROP will only accept 100 observations, an attempt was made to determine orbits from observations extending over only about 3 hours (2 revolutions). However, these orbits proved to be unreliable because the observations were concentrated at a small number of stations with inadequate geographical distribution, leading to geometrical bias. Also the orbital period and its rate of change were ill-defined, because the time interval of the observations was too short, and the drag was so high that M_2 could not be omitted from the model.

So the time interval was extended to 12 hours - before and after midnight. This meant that two thirds of the observations had to be omitted, and this was accomplished by reducing the number of observations per transit at each station. At some stations there were more than 20 observations per transit so the removal of two thirds was not serious. The two sets of elements obtained are given in Table 2 as 13A and 13B with the standard deviations below each value: the first orbit, 13A, is determined from observations before midnight (July 10.0) and the second, 13B, from observations after midnight. A third orbit was determined from observations taken from both 13A and 13B at times within 6 hours of the epoch, July 10.0. This orbit is given as orbit 13C in Table 2.

The agreement between the three orbits at epoch July 10.0 is very good. The values of eccentricity, e, and argument of perigee, ω, agree to within their standard deviations, the three values of inclination, i, are within twice the sum of their standard deviations, and the values of right ascension of the node, Ω, within three times the sum of their standard deviations. The values of M_1 (and hence semi major axis, a) and M_2 however do not agree so well. This is because orbits 13A and 13B are determined from observations away from epoch and therefore experience different drag conditions. Since the model (for orbit 13) does not include M_3, the values of M_2 in

Table 2

Values of the orbital parameters, with standard deviations, for orbits 13 to 15

	MJD	Date 1979	a	e	i	Ω	ω	ω + M_0	M_1	M_2	M_3	Time span of observations	ε	N	D	a − 6372
13A	44064	July 10.0	6560.387 5	0.000182 3	50.0174 4	342.7663 5	347.2 1.0	37.190	5881.285 7	8.972 14	-	12 h 18 m to 22 h 44 m on July 9	0.25	98	0.43	188.39
13B	44064	July 10.0	6560.615 11	0.000186 6	50.0164 5	342.7665 4	346.7 1.1	37.231	5880.978 14	11.695 23	-	01 h 56 m to 11 h 49 m on July 10	0.40	100	0.41	188.62
13C	44064	July 10.0	6560.234 1	0.000182 3	50.0161 3	342.7685 3	346.3 9	37.204	5881.490 2	9.584 10	-	18 h 03 m on July 9 to 04 h 15 m on July 10	0.23	94	0.43	188.23
14A	44065	July 11.0	6539.759 34	0.000192 2	50.0152 2	336.9368 3	333.1 9	175.736	5909.129 46	19.082 186	3.80 23	13 h 20 m to 20 h 54 m on July 10	0.22	83	0.32	167.76
14B	44065	July 11.0	6539.779 51	0.000192 3	50.0154 3	336.9400 3	331.0 1.0	175.764	5909.101 69	23.438 531	7.02 1.12	01 h 23 m to 06 h 53 m on July 11	0.18	48	0.23	167.78
14C	44065	July 11.0	6539.512 4	0.000206 4	50.0134 5	336.9385 5	331.6 1.3	175.748	5909.463 5	21.486 43	8.94 18	17 h 56 m on July 10 to 04 h 23 m on July 11	0.47	99	0.43	167.52
14D	44065	July 11.0	[6507.524 547]	0.000222 10	50.0124 10	336.967 2	331.6 2.1	169.746	[5953.083 0.750]	-84.39 1.59	96.6] 1.1]	08 h 08 m to 16 h 02 m on July 11	0.66	98	0.33	-
15	44065.5	July 11.5	6516.237	0.000195	50.0094	333.984	334.1	259.737	5941.153	60.53	96.6	08 h 08 m to 16 h 02 m on July 11	(Converted from 14D)			144.24

Key:
- MJD = modified Julian day
- a = semi major axis (km)
- e = eccentricity
- i = inclination (deg)
- Ω = right ascension of ascending node (deg)
- ω = argument of perigee (deg)
- M_0 = mean anomaly at epoch (deg)
- M_1 = mean motion n (deg/day)
- M_2, M_3 = later coefficients in the polynomial for M
- ε = measure of fit
- N = number of observations used
- D = time covered by the observations (days)

orbits 13A and 13B are those appropriate over the time interval of the observations, centred at July 9.7 and July 10.3 respectively. The value of M_2 for orbit 13C should be that appropriate to July 10.0, being derived from observations over the epoch, and the value of M_1 on orbit 13C should be taken as correct, since the values on orbits 13A and 13B are extropolated using values of M_2 derived from the fitting of observations away from epoch.

2.3 For July 11.0

On the morning of July 11 at 07.45 UT Skylab was commanded to manoeuvre to a tumble attitude, thus reducing the drag and extending the lifetime. This action was taken to shift the probable impact footprint away from the highly populated east coast of the United States and Canada to the Indian Ocean[6]. Therefore the 800 observations available between midday on July 10 and decay were divided into three groups: about 400 between 12.00 h and midnight on July 10; about 90 between 00 h and the manoeuvre at 07.45 UT on July 11; and finally some 300 observations between 07.45 UT and decay.

For the orbits derived from the first two sets of observations, 14A and 14B, at epoch July 11.0, it was necessary to alter the orbital model, because the eccentricity increased slightly between July 9.0 and July 11.0 (due to the day-to-night variation in air density), whereas the PROP model indicates a decrease in accordance with the theory for decay in a spherically symmetrical atmosphere. At July 11.0 the rate of change of e per day given by the model was strongly negative (-0.00011 for 14A and -0.00016 for 14B), and an appropriate positive $\dot{e}$ was added to the model to give consistent results. The method chosen was to adjust the added $\dot{e}$ so as to give identical values of e on the two orbits: the added $\dot{e}$ was 0.00010 on both, giving $\dot{e}$ on the (modified) model as -0.00002 for 14A and -0.00005 for 14B. (These values are different because the values of M_2 are different.) This procedure adopted for 14A and 14B was not necessary on orbits 13A and 13B, presumably because the rate of decrease of e in the PROP model was much smaller (being proportional to M_2).

The sets of elements for orbits 14A and14B are given in Table 2. A third orbit was determined from observations, taken from 14A and 14B, over the epoch, July 11.0. For this orbit, 14C, the observations ranged from 17.56 UT on July 10 to 04.23 on July 11. The orbital elements for orbit 14C are given in Table 2. Comparing the three sets of elements for July 11.0, orbits 14A, B and C, we see that the values of M_1, M_2 and M_3, and hence a, are much more accurately determined for orbit 14C, and this is probably due to the wider spread of the observations in time and perhaps in latitude, and the fact that they cover the epoch. Comparing the values of e, i and Ω on orbit 14C with those on orbits 14A and 14B it can be seen that they agree to within 2.3 times the sum of their standard deviations. The values of M_2 on orbits 14A and 14B differ and, as before, may be taken as applying at a time midway through the observations rather than at July 11.0.

In the analysis to follow, the orbits 13C and 14C have been used for July 10.0 and 11.0 respectively.

2.4 For the last eight hours (08.08 to 16.02 UT) on July 11

The observations available after the tumble action at 07.45 UT on July 11 have been used to derive one further orbit. As the epoch at which the orbit is determined by the PROP program is always at 00 h, the observations were being fitted away from epoch. So, besides giving the orbit determined at 00 h as 14D in Table 2, the elements have been converted to midday to give an orbit 15 for July 11.5. Orbit 15, with an epoch in the midst of the observations, is obviously preferable for use in any further analysis.

There was a difficulty with the convergence process in the PROP program for this last orbit (14D), and results could only be obtained by fixing the value of e and allowing the other parameters to change. After this another PROP fitting was run keeping all the values determined on the previous run fixed, but leaving e free to be determined. However, the change in e was negligible, only 1×10^{-6}. There was still the problem of estimating the value of the standard deviation for e. This was done by comparing the standard deviations printed out on runs which had not converged but had reached the same value of ε as the run with e fixed. On this basis the standard deviation for e was estimated as 10×10^{-6}.

Although orbit 14D is at an epoch well outside the time span covered by the observations, the values of e, i, Ω and ω are surprisingly good. The values of M_0, M_1 (and a) and M_2 on orbit 14D look peculiar, but this is merely because they are coefficients of a polynomial with an inappropriate zero point, and, when converted to epoch July 11.5, they give reasonable values. These values in orbit 14D have been enclosed in square brackets to emphasize their inappropriate character.

The accuracy of orbit 15 cannot be formally assessed because of the convergence problem on 14D, but since a good value of ε was achieved (only 40% higher on 14D than on 14C), it would be surprising if the main orbital parameters (*ie* excluding M_0, M_1 and M_2) had errors more than twice as large as 14C. However, the errors are likely to be larger than on 14C. Thus the standard deviations on 14D seem suitable for use on orbit 15.

3 ANALYSIS OF THE INCLINATION

3.1 Treatment of the data

The values of inclination on the 15 orbits from Tables 1 and 2, with their standard deviations, are plotted in Fig 2. The values for orbits 13 and 14 are taken from the orbits from observations over the epoch - namely 13C and 14C. The general decrease due to the effect of atmospheric rotation is visible, but all other perturbations must be removed before an analysis can be attempted and a value of the upper-atmosphere rotation rate, Λ, determined.

Fig 3 gives the values of inclination plotted against date after removal of the zonal harmonic, $J_{2,2}$ and lunisolar perturbations. The zonal harmonic and lunisolar perturbations were removed by using the PROD computer program[7] with 1-day integration steps, and the $J_{2,2}$ tesseral harmonic perturbation by using the value recorded with the PROP printout.

During the 14 days of the analysis the perturbation in inclination due to earth and ocean tides[8] should not build up to more than 0.0001° (10 metres) and can therefore be absorbed in any standard deviations of 0.0003° or greater; however the three standard deviations of 0.0002° are increased to 0.0003°, to allow for neglect of earth and ocean tide effects, and this increase is shown in Fig 3. Similarly the estimated change in inclination in 14 days due to solar radiation pressure[9] is less than 0.0001°, and can also be absorbed in the standard deviation.

There remains one source of perturbations which cannot be adequately modelled. Because of the peculiar shape of Skylab 1, Fig 1, there is a possibility of aerodynamic forces perpendicular to the orbital plane, which may perturb the inclination enough to degrade the accuracy of the determination of wind speed. This is discussed in section 3.5.

3.2 Analysis of the variation of inclination with time

The theoretical variation of inclination due to atmospheric rotation and meridional winds can be calculated for a series of values of Λ, and of μ, the south-to-north atmospheric rotation rate, using a computer program (ROTATM) based on equations (32) and (33) of Ref 10.

The variation was computed for values of Λ from 1.0 to 1.35 rev/day at intervals of 0.05 with $\mu = 0$ and 0.1 rev/day. The addition of the $\mu = 0.1$ term had no effect. This was not surprising because a constant south-to-north wind has no effect on the inclination of a circular orbit[11]. Even with a non-circular orbit, the variation in inclination due to meridional rotation is proportional to $\cos \omega$, and here ω is near 90° until after orbit 10 on July 7; during the last 4 days ω changes from 53° to 332° and the local time is 04 ± 3 h, when the meridional wind is normally towards the equator, and as perigee moves from north to south of the equator the effect of the wind would tend to cancel out. So there is no reason to suppose that meridional winds are of any importance here.

The values of inclination were therefore fitted by choosing the best value of Λ, assuming $\mu = 0$. The best fit between theory and the observational values of inclination was difficult to decide, but appears to be with Λ between 1.20 and 1.30. The theoretical curve for $\Lambda = 1.25$ has therefore been drawn through the points in Fig 3. In order to assess the likely errors in the values of Λ, a realistic estimate of the likely errors in i at the beginning (i_B) and end (i_E) of the curve, σ_B and σ_E, was made, and then $\Lambda\sqrt{\sigma_B^2 + \sigma_E^2}\,/(i_B - i_E)$ was taken as the standard deviation in Λ. This was found to be 0.11.

The value of $\Lambda = 1.25 \pm 0.11$ obtained from fitting the values of i in Fig 3, can be regarded as averaged in local time because the orbit is so nearly circular. The height decreases from 253 km to 147 km during the 13½ days, and the average height at which Λ applies is difficult to determine. In the Appendix an attempt is made to derive as logical as possible a value for the mean height, based on averaging the air density. This method gives a mean height of 211 km, but the omission of orbit 15 alters

the mean height to 218 km, while still yielding the same value of Λ. So the mean height should perhaps be regarded as a height band of 210 to 220 km, rather than an exact value.

The value of Λ is larger than might be expected from Fig 13 of Ref 12, where a value of 1.1 for Λ is indicated for a satellite at 210 to 220 km height in 'average' conditions.

3.3 Analysis of inclination in terms of orbital period

For satellites in near-circular orbits, with eccentricity less than 0.005, the change Δi in inclination produced by a change ΔT_d in orbital period can be expressed much more simply than in the lengthy theoretical equation of Ref 10. The simplified form is

$$\frac{\Delta i}{\Delta T_d} = \frac{\Lambda \sin i}{6\sqrt{F'}}\left\{1 + \tfrac{1}{2}c + O\left(\frac{z^2}{8}\right)\right\} \quad , \qquad (2)$$

where $z = ae/H$ is of order 0.1. The parameter c allows for the effect of atmospheric oblateness and

$$c = \frac{\varepsilon' a(1 - e) \sin^2 i}{2H} \quad ,$$

where ε' is the ellipticity of the atmosphere (taken as 0.00335) and H is the density scale height. The factor F' in equation (2) is given by $\sqrt{F'} = 1 - \{a(1 - e)w \cos i\}/V_p$, where V_p is the satellite's velocity at perigee and w is the angular velocity of the atmosphere near perigee. So, if Λ is constant, the values of inclination for a circular-orbit satellite, when plotted against orbital period, should lie on a straight line whose slope gives the value of Λ.

Here the eccentricity of Skylab is below 0.001, so this method should yield a good determination of Λ. The values of inclination, with perturbations removed, are plotted against anomalistic period in Fig 4 and a least-squares fitted straight line to the values of inclination has a slope of 0.0074 ± 0.0005 deg/min. For this satellite, with $c = 0.186$ and $F' = 0.908$, equation (2) gives $\Lambda = 1.28 \pm 0.09$. This is consistent with the value found in section 3.2, namely $\Lambda = 1.25 \pm 0.11$. But the fitting is not as good as might be hoped, the measure of fit ε being 2.5.

3.4 16th-order resonance

As the values of Λ obtained in sections 3.2 and 3.3 are larger than might have been expected, and the fitting fell short of expectations, it was natural to look for any other perturbation that might affect the values of inclination. With this in mind, the 16th-order resonance was investigated. Previously it had been assumed that the satellite would pass through 16th-order resonance very quickly and that no change in inclination would be discernible. The date of resonance was July 8.9, three days before decay. In the past we have normally limited the range of $\dot{\phi}$, the rate of change of the resonant angle, to ±20 deg/day when the orbits available over the resonant period were 7 days apart. Here the analysis can be extended to a much larger value of $\dot{\phi}$, as the orbits are daily and the range of ϕ over which the resonance is analysed will be

The theory for the rate of change of inclination at resonance is given in section 5.1 of Ref 10 where the parameters used are defined. The first term, *ie* the $(\gamma,q) = 0$ term, in the equation for rate of change of inclination near 16th-order resonance is

$$\frac{di}{dt} = \frac{n}{\sin i}\left(\frac{R}{a}\right)^{17}(16 - \cos i)\bar{F}_{17,16,8}\left\{\bar{S}_{16}^{0,1}\sin\Phi + \bar{C}_{16}^{0,1}\cos\Phi\right\}, \qquad (3)$$

where $\Phi = \omega + M + 16(\Omega - \nu)$ is the resonance angle, ν being the sidereal angle.

The values of inclination, cleared of zonal harmonic, $J_{2,2}$ and lunisolar perturbations, were fitted with equation (3), in integrated form, using the THROE computer program[13]. The first fitting was made with $\Lambda = 1.20$ and ε, the measure-of-fit parameter, was 2.36. Three of the worst-fitting values, with weighted residuals over 3.0, were then degraded by a factor of 2 and the resulting lumped coefficients were:

$$10^9\bar{C}_{16}^{0,1} = 149 \pm 44 \qquad 10^9\bar{S}_{16}^{0,1} = -34 \pm 37$$

with $\varepsilon = 1.65$.

The values of inclination could now also be cleared of the resonance perturbation and a straight line was fitted to the values by least squares, as in section 3.3. This straight-line fit gave a value of $\Lambda = 1.12 \pm 0.05$. As this was considerably different from the value of Λ used in the THROE fitting, the program was re-run with $\Lambda = 1.10$. This yielded the following values of lumped coefficients:

$$10^9\bar{C}_{16}^{0,1} = 147 \pm 42 \qquad 10^9\bar{S}_{16}^{0,1} = 4 \pm 35$$

with $\varepsilon = 1.56$ after one further value was degraded by a factor of 2 to bring all the weighted residuals below 2.5. The fitted curve is plotted in Fig 5.

The values of inclination were again cleared of the resonance perturbation using this revised fitting of equation (3) with $\Lambda = 1.10$ and the resulting values fitted with a least-squares straight line. The two values of inclination for July 10 and July 11 had their standard deviations increased for this fitting by a factor of 2. The resultant value of Λ was 1.10 ± 0.07, and the straight-line fit to the values of inclination is shown in Fig 6.

So the value of Λ obtained from the straight-line fit to the values of inclination is now consistent with the value used in the THROE fitting. The higher values of Λ obtained in sections 3.2 and 3.3 occur because there is a decrease in inclination due to resonance of approximately 0.002°, as well as the decrease in inclination due to atmospheric rotation.

3.5 Discussion

The value of Λ obtained from the straight-line fitting to the values of inclination, after allowing for the resonance, is obviously preferable. However, the

values of inclination in Fig 6 do not fit the straight line quite as well as might be expected, and the parameter ε indicating the measure of fit had a value of 1.4 despite the relaxation of a number of values. The high value of ε probably means that the standard deviations obtained for the inclination from the PROP runs are too low - they are equivalent to about 40 m. Previous values of inclination for other satellites evaluated from similar observations have yielded standard deviations about twice as large[10,14,15]. The low standard deviations probably arise as a result of bias and over-fitting to long runs of observations from the same station, and 60 to 70 m is probably a more realistic figure than 40 m. An extreme example of such bias is the orbit for June 27 in Table 1, which was subsequently ignored because it was based on only 25 observations from only five stations. In this orbit the value of inclination appears to have a bias error of about 0.0067°, compared with a standard deviation of 0.0038°.

Because of the unusual shape of Skylab, the possibility arises of aerodynamic forces perpendicular to the orbital plane; but these would probably be averaged over each revolution and would not then affect these orbits determined over several revolutions. As the fitting of the line in Fig 6 is not perfect, it is possible that the lateral aerodynamic forces had an appreciable effect causing a decrease in inclination at a period of about 88.8 min and an increase at a period near 88.3 min. However this seems rather unlikely, since the spacecraft attitude was maintained in a fixed mode[6] during this time. The alternative explanation already given, of the standard deviations being too low, is therefore to be preferred.

The fitting of the variations in inclination at 16th-order resonance is the first successful analysis of its kind. Previously all attempts to analyse 16th-order resonance had been thwarted by the high drag and the satellite's rapid passage through resonance. The analysis has succeeded with Skylab 1 because (a) the orbit is circular, thus minimizing drag for given orbital period, (b) the mass/area is large, and (c) numerous accurate observations were available, thus enabling accurate orbits to be determined.

It is of interest to compare the values of the lumped 16th-order coefficients obtained from Skylab 1 with those given by comprehensive geopotential models. The best of these is the Goddard Earth Model, GEM 10B [16], which extends to order and degree 36; the terms of degree $\ell > 36$ can be taken from GEM 10C, which goes to degree and order 180. The lumped value $\bar{C}_{16}^{0,1}$, for Skylab 1 at 50.0° inclination, can be expressed in terms of the individual values, $\bar{C}_{\ell,16}$, by the following equation

$$\begin{aligned}\bar{C}_{16}^{0,1} = {} & \bar{C}_{17,16} - 3.91\bar{C}_{19,16} + 6.70\bar{C}_{21,16} - 4.73\bar{C}_{23,16} - 1.46\bar{C}_{25,16} + 4.18\bar{C}_{27,16} \\ & - 0.12\bar{C}_{29,16} - 3.26\bar{C}_{31,16} + 0.44\bar{C}_{33,16} + 2.62\bar{C}_{35,16} - 0.34\bar{C}_{37,16} \\ & - 2.17\bar{C}_{39,16} + \text{terms of degree} > 40 \quad ,\end{aligned}$$

and similarly for S, on replacing C by S throughout. If the standard deviations of the individual coefficients from GEM 10B (and C) are taken[17] as 3×10^{-9}, the lumped values are as given below

	from Skylab	from GEM 10B/C
$10^9 \bar{C}^{0,1}_{16}$	147 ± 42	117 ± 34
$10^9 \bar{S}^{0,1}_{16}$	4 ± 35	35 ± 34 .

The agreement is very satisfactory and suggests the values from both sources are reliable to within their quoted standard deviations.

4 DETERMINATION OF AIR DENSITY FROM DECAY RATE

4.1 Theory

Daily decay rates can be obtained from the orbits in Tables 1 and 2, and the density of the atmosphere at a mean height can be calculated at daily intervals. The density ρ at a radial distance $\bar{a}$, the 'mean' distance at which the density values apply, can be obtained by substituting $\dot{T} = 3\pi(a/\mu)^{\frac{1}{2}}\dot{a}$ in equation (7.10) of Ref 18 to give

$$\rho = - \frac{\Delta a/\Delta t}{(\mu\bar{a})^{\frac{1}{2}}\delta\{1 + \tfrac{1}{4}c^2\}} ,$$

where Δa is the change in a in one day. Since $\mu^{\frac{1}{2}} = 631.35 \text{ km}^{\frac{3}{2}} \text{ s}^{-1}$ and $\Delta t = 86400$ s here,

$$10^9\rho = - \frac{\Delta a}{54.55\delta(\bar{a})^{\frac{1}{2}}\{1 + \tfrac{1}{4}c^2\}} , \qquad (4)$$

where Δa and $\bar{a}$ are in kilometres, the area/mass parameter δ is in m^2/kg and ρ is in kg/m^3. (The values of Δa are given in Fig 17.)

Equation (4) includes the effect of atmospheric oblateness but does not allow for the day-to-night variation in air density. If f is the ratio of maximum daytime density to minimum night-time density and $F = (f - 1)/(f + 1)$, equation (39) of Ref 19 includes the effect of day-to-night variation in air density and, with $r_0 = a$, gives

$$\frac{\Delta a}{\Delta t} = - (\mu a)^{\frac{1}{2}}\rho\delta I_0\left[1 + \tfrac{1}{2}F\left(1 - \frac{I_2}{I_0}\right)z(P \sin\omega + Q \cos\omega) + O(e,F^2)\right] , \qquad (5)$$

where I_n is the Bessel function of the first kind and imaginary argument of degree n and argument z, and P and Q are direction cosines. Here $F < 0.22$ and $z < 0.136$, so that I_0 may be taken as 1.0 with error less than 0.5%, and the $\frac{1}{2}F$ term in equation (5) is less than 0.015. Thus equation (5) reduces to the form appropriate for $F = 0$ and $e = 0$, with error <1.5%, and equation (4) can be used, as it is the same as the reduced form of equation (5), except that the effect of atmospheric oblateness, expressed through the parameter c, is added.

The 'mean' distance $\bar{a}$ at which the values of density apply is given by

$$\beta(a_0 - \bar{a}) = \ln\left[\frac{\beta(a_0 - a_1)}{1 - \exp\{-\beta(a_0 - a_1)\}}\right] , \qquad (6)$$

where a_0 and a_1 are the values of a from Tables 1 and 2 one day apart appropriate to each daily value of density, and $\beta = 1/H$. If $\beta(a_0 - a_1)$ is small, equation (6) reduces to

$$\frac{a_0 - \bar{a}}{a_0 - a_1} = \frac{1}{2} - \frac{\beta(a_0 - a_1)}{24} + O\left[\frac{1}{60}\left\{\beta(a_0 - a_1)\right\}^3\right] . \qquad (7)$$

For the derivation of equations (6) and (7), see the Appendix.

4.2 Results

Values of density were determined at daily intervals using equation (4) with appropriate daily values of $\bar{a}$. The value used for δ, the area/mass parameter, was taken from Ref 6 as 7.692×10^{-3} m^2/kg. The values of density ρ are plotted as circles at the top of Fig 7, the values of the solar activity index $S_{10.7}$ and the daily planetary geomagnetic index Ap being indicated below. The exospheric temperature T_∞ appropriate for each day, according to the COSPAR International Reference Atmosphere 1972 [20] (*CIRA 1972*), has been calculated taking account of the values of $S_{10.7}$ and Ap for that day, and the values of density have been standardized to a value of exospheric temperature of 1110 K, by multiplying the density values ρ by a factor G, given by $G = \rho(1110)/\rho(T_\infty)$, where the values of $\rho(1110)$ and $\rho(T_\infty)$ are obtained from the *CIRA* tables at the appropriate height. The values of G are plotted at the bottom of Fig 7 and it can be seen that the adjustment for solar and geomagnetic activity is as much as 15% on some days. The decrease in G between June 29.5 and July 4.5 reflects the increase in $S_{10.7}$ at this time; the increase in G between July 7.5 and July 10.5 is partly due to a decrease in $S_{10.7}$ and Ap, but also partly because the satellite has descended to a height where the effects of solar activity are smaller.

The adjusted values of density ρ^* ($= G\rho$) are plotted against height y in Fig 8. The height is given by $y = \bar{a} - \bar{R}$, where $\bar{R}$ is the mean Earth radius, $\bar{R} = R(1 - \frac{1}{2}\epsilon' \sin^2 i)$, calculated here to be 6372 km. The values of $\bar{a}$ are obtained from either equation (6) or (7) at the time of each daily evaluation of ρ^*.

The curves in Fig 8 are plotted from *CIRA 1972* for three values of exospheric temperature, 900 K, 1000 K and 1100 K. The values of ρ^*, which were standardized to a value of exospheric temperature of 1110 K, lie in a band centred on $T_\infty = 1025$ K. This reduction in T_∞ is to be expected because all these values of ρ^* apply at a time near the July semi-annual minimum in density. In terms of density, the observational values are below the *CIRA* 1110 K standard by an average of 15% for the first eight values, evaluated between 226 and 251 km, and an average of 9% for the remaining five values, at heights of 179 to 221 km. The semi-annual variation given in *CIRA 1972* indicates a decrease of 14% at a height of 250 km on June 29 and a decrease of 13% at a height of

200 km on July 9. The values from the analysis thus agree well with those of *CIRA 1972*, within 1% for June 28 to July 6 and within 4% for July 7 to 11. This indicates that the semi-annual variation in July 1979 conforms to that specified by the *CIRA* model. This result is different from that obtained for the early 1970s [21] from analysis of 1971-106A, which indicated a 20% reduction in density for early July due to the semi-annual variation. However, the semi-annual variation changes from year to year[21], and it appears that the variation in July 1979 conformed to *CIRA 1972*, which is based on results in the 1960s.

In a recent paper Eisner and Yionoulis[22] find that the semi-annual variation in 1975 to 1978, at heights of 900 to 1200 km, has a smaller amplitude than that in Jacchia's 1977 model[23], which is very similar to that of *CIRA 1972*. Their results, together with those obtained here, suggest that the amplitude of the semi-annual variation in the late 1970s was smaller than in the early 1970s.

5 ANALYSIS OF ECCENTRICITY AND ARGUMENT OF PERIGEE

5.1 Variation of eccentricity with time

The values of eccentricity e for the 15 orbits in Tables 1 and 2 are plotted in Fig 9. As with the inclination, the values for July 10.0 and 11.0 are from orbits 13C and 14C.

The decrease of eccentricity due to drag in an atmosphere with day-to-night variation in density, with a day-time maximum density 'bulge' at 14 h local time, is given by equation (32) of Ref 24 as

$$\Delta e = - K\left\{I_1 + \tfrac{1}{2}FI_0 \cos \phi_p + O(e, \tfrac{1}{2}z^2)\right\} \quad , \tag{8}$$

where K is a positive constant for each epoch and ϕ_p is the bulge-perigee angle. Here z is small, of order 0.1, so $I_0 \approx 1.0$ and $I_1 \approx \tfrac{1}{2}z$; therefore equation (8) may be written as

$$\Delta e = - \tfrac{1}{2}K\left\{z + F \cos \phi_p + O(e, \tfrac{1}{2}z^2)\right\} \quad . \tag{9}$$

Between June 28 and July 5, the value of F is near 0.2 and ϕ_p is between 24° and 36° (see Fig 12), so that $0.81 < \cos \phi_p < 0.91$; hence $F \cos \phi_p$ is slightly greater than z , and e should decrease much more rapidly as a result of the day-to-night variation in density. The broken curve in Fig 9 shows the theoretical decrease of e in an atmosphere without day-to-night variation, and the actual decrease is much steeper, as predicted by the theory, between June 28 and July 5.

Between July 6 and July 11, ϕ_p increases steadily from 42° to 178° (see Fig 12), and $\cos \phi_p$ becomes negative after July 8, thus making $z + F \cos \phi_p$ negative for July 9 to 11. Therefore an increase in e is to be expected at this time, as is seen in Fig 9.

The day-to-night variation in density becomes very small below 190 km, with $F < 0.1$, and so e would be expected to decrease in the last 12 hours of the life in accordance with the spherical-atmosphere theory, and the last orbit shows that this is beginning to occur.

5.2 Variation of eccentricity with argument of perigee

When the eccentricity is so small (<0.001) and the drag so large, the argument of perigee, ω, no longer undergoes its regular variation with time, controlled by the gravitational effects of the Earth's oblateness; instead the gravitational effects become subordinate to the effects of the day-to-night variation in air density.

In the absence of air drag the variation of e and ω would be a circular path in the ($e \cos \omega$, $e \sin \omega$) plane, the centre of the circle being on the $e \sin \omega$ axis at a distance which, for $i = 50.0^\circ$ and $a = 6625$ km, is 0.84×10^{-3}. In Fig 10 the set of points plotted as crosses shows the variation in e that would occur during the 14 days of the orbit determination in the absence of drag, as given by PROD[7]: as expected, the form is a circle centred near the point (0, 0.84), with small departures from the circle caused by lunisolar perturbations. The actual values of e and ω, also shown in Fig 10, follow a very different course, with very large changes in ω near the end of the life, as shown in Fig 11. To discover the reason for this unusual variation, it is necessary to consider the theory for decaying near-circular orbits in an atmosphere with day-to-night variation in density[19].

In the theory it is assumed that the maximum daytime density is at 14 h local time and the minimum night-time density at 02 h local time, both on the equator. (This is an approximation made in the theory; the maximum would actually be north of the equator in June and July.) The theory[19] is developed in terms of $z = ae/H$ (with constant H), and shows that, as decay approaches, z tends to approach the value $z_F = |F \cos \phi_p|$ and ω tends to approach the value $\omega_F = \tan^{-1}(-\cos i \tan M')$, where $M' = \Omega - L - 30^\circ$ and L is the solar longitude. Also the value of the bulge-perigee angle ϕ_p tends towards the value ϕ_{pF}, where

$$\cos \phi_{pF} = -\left\{1 - \sin^2 i \sin^2 M'\right\}^{\frac{1}{2}} \quad . \tag{10}$$

The values of ϕ_{pF} for each day of the orbit determination are shown in Fig 12, together with the actual values of ϕ_p. Between June 28 and July 4, the impression is that ϕ_p is making no attempt to approach ϕ_{pF}, and this is not surprising since the drag is not severe enough at this stage to cause the perigee to swing round towards the point of minimum density, as predicted by the theory. After July 4, however, the drag takes command and ϕ_p rapidly approaches ϕ_{pF}, nearly coinciding with it at the end (the difference being within the errors caused by assuming an equatorial position for the maximum and minimum densities).

The values of z_F and ω_F have also been calculated for each day of the orbit determination, and they are plotted as triangles in the ($z \cos \omega$, $z \sin \omega$) plane in Fig 13. The corresponding observational values of $z \cos \omega$ and $z \sin \omega$ are plotted as circles, the numbers indicating the orbit number in Tables 1 and 2.

Fig 13 can be interpreted satisfactorily in the light of the theory, which suggests that the observational values should be moving towards the appropriate triangles as soon as the drag is strong enough to overcome the effects of the gravitational field. For

orbits 1 to 5 the initial direction of motion under the influence of the gravitational field is still maintained, though it also happens to be in the direction required by the minimum-density criterion, *ie* the values shown as circles are heading towards the appropriate triangles. For orbits 6 to 10, when the day-to-night variation in density exerts more influence, the observed values of z head straight towards the appropriate z_F values. For orbits 10 to 12, z_F moves rapidly to zero and out again, and the observed values of z head towards the values of z_F, ignoring the short-lived excursion of z_F to zero. After orbit 13 the height of the satellite has decreased to below 190 km where the day-to-night variation is much smaller, with $F < 0.1$, so the tendency for z to approach z_F grows slightly weaker, while there is an increasing tendency for e to decrease due to the basic spherical-atmosphere drag.

At this stage it becomes preferable to interpret the results in terms of e rather than z. So far it has been possible to treat z (= ae/H) and e as similar, because the change in H between one orbit and the next has not been large enough to invalidate the assumption of constant H in the theory. But for orbits 12 to 15 there are substantial changes in H, and so it is better to consider $e_F = Hz_F/a$ (where H/a has separate values for each orbit) and to look at the variation of e relative to e_F. The values of e and e_F on orbits 12 to 15 are shown on the inset diagram in Fig 13. In the last three days the value of ω_F slowly increases from 335° to 350°. The actual value of ω is rapidly decreasing between orbit 12 and orbit 13, but then slows down between orbits 13 and 14 (see Fig 11) as it has overshot the value of ω_F, and increases between orbits 14 and 15. On orbits 12 and 13, $e < e_F$ and so e would be expected to increase, and does so. Between orbits 14 and 15, e_F becomes less than e, and the slight decrease in e on orbit 15 reflects this. Thus the theory is fully borne out by the observed variation.

5.3 Analysis of perigee position

Having established that the movement of perigee is in conformity with the theory, it is worth looking at the motion of the perigee point in more detail, to examine its progress towards the minimum-density point, while remaining within the orbital plane.

Fig 14 gives sketches showing how this progress develops. Fig 14a defines the notation: P is the actual perigee position; D is the point of minimum density (assuming an equatorial Sun, as in the theory); and P_F is the 'final' value of perigee towards which perigee should be moving according to the theory, *ie* the point of minimum density in the orbital plane.

Fig 14b-e illustrate the movement of P on four selected orbits, Nos. 1, 4, 10 and 14. Initially, Fig 14b, P is near northern apex ($\omega = 120^\circ$) and ω is slowly increasing due to the gravitational field. At this time P is at local time 16 h. By orbit 4 the argument of perigee has ceased to increase and the effect of the day-to-night variation in air density gradually begins to take command over the effect of the gravitational field. However, the perigee happens to be close to the maximum-density point on orbits 1 to 4, and so at this stage P has a long way to go to reach P_F. In orbit 10, shown in Fig 14d, P is rapidly moving towards P_F, the minimum-density point

in the orbital plane. Finally, in Fig 14e, a sketch of orbit 14, the perigee position has slightly overshot the position of P_F . (However, as stated previously, the angular separation of P and P_F is within the errors caused by assuming an equatorial position for the Sun.)

6 THE REMAINING ORBITAL ELEMENTS

6.1 The semi major axis

The values of semi major axis a from Tables 1 and 2 are plotted as circles in Fig 15 and joined by a smooth curve (full line). They are plotted against t'/t_L where t' is the time in days after June 28.0 and t_L is the lifetime from June 28.0, *ie* 13.69 days.

The dashed curve in Fig 15, determined from equation (4.90) of Ref 18, gives the theoretical change in a over the same interval as the orbit determinations, assuming no variation of density with time and a constant density scale height H . If a_0 is the initial value of a (6624.9 km), equation (4.90) may be written

$$\frac{t'}{t_L} = \frac{1}{\eta}\left[1 - \exp\left\{-\frac{(a_0 - a)}{H}\right\}\right] \quad , \tag{11}$$

where $\eta = 1 - \exp\{-(a_0 - a_L)/H\}$ and a_L , taken as 6472 km, is the value of a at decay. Equation (11) applies for a spherical or oblate atmosphere.

The dash-dot curve gives a nearer approximation by allowing for a variable scale height, as in equation (6.81) of Ref 18, where the symbol μ represents the rate of increase of H with height and the variation of a with t' is given by

$$\frac{t'}{t_L} = \frac{1}{\eta}\left[1 - \exp\left\{-\frac{(a_0 - a)}{H_8}\right\} + \tfrac{1}{2}\mu U + O(\tfrac{1}{2}\mu^2)\right] \quad . \tag{12}$$

Here H_8 is the value of H at one scale height below the initial height (*ie* at a distance $a_0 - H_8$ from the Earth's centre), η is calculated with $H = H_8$, ($\eta = 0.986$ here), and U is a function of t'/t_L plotted in Fig 6.5 of Ref 18.

In the theory it is assumed that $\mu < 0.2$. Here *CIRA 1972* indicates that μ is 0.2 on June 28 and increases to 0.35 on July 11, and a 2% error in t' is introduced by limiting μ to 0.2. There is also an error due to the neglect of terms of order $\frac{1}{2}\mu^2$ in equation (12), which is 0.02 if $\mu = 0.2$.

Even with the limitations of equation (12), however, the dash-dot curve gives a better approximation to the true decrease in semi major axis than the constant-H equation (dash curve). The maximum departure of the actual t'/t_L from the theoretical value is 4% with equation (11) and 2% with equation (12). This is well within the expected error due to neglect of μ^2 and variations of density with time.

6.2 The right ascension of the ascending node

The values of right ascension of the ascending node, Ω , are plotted in Fig 16 against date and they follow the expected pattern, decreasing by about 5.7 deg/day due to

the effect of the even zonal harmonics in the geopotential. If there was any variation in Ω due to atmospheric rotation, the perturbations due to the even zonal harmonics and lunisolar forces would first have to be removed, and then the residual variation fitted with[18]

$$\frac{\Delta\Omega}{\Delta T_d} = \frac{\Lambda \sin 2\omega}{6\sqrt{F'}}\left[\frac{I_2}{I_0}\left\{1 - 2e\frac{I_1}{I_2}\left(1 + \frac{I_2}{I_0}\right) + O(e^2)\right\}\right] . \qquad (13)$$

Here, $I_2/I_0 < 0.003$ because $e < 0.001$ and $z < 0.136$, and the effect would be negligible. So it is not possible to determine Λ from the variation of Ω.

6.3 The orbital decay rate

Fig 17 shows as circles the orbital decay rates $\dot{n}$ $(= 2M_2)$ in deg/day^2 for the orbits of Tables 1 and 2, the values for the orbits 13A and B and 14A and B being plotted at times away from epoch, for the reasons given in section 2. These values of $\dot{n}$ could have been used to determine values of density, but they are instantaneous values, and the method preferred (section 4) was to use the average daily change in semi major axis Δa to give daily values of $\dot{a}$ $(= \Delta a/\Delta t)$. These values of Δa are also plotted in histogram form in Fig 17.

Although the two sets are not strictly comparable, they should of course show the same trends. The means of the successive daily values of Δa, which represent the mean drag over 2 days, are joined with a broken line up to July 9 and this closely parallels the unbroken curve. The ratio of $2M_2$(deg/day^2)/Δa(km) should be 1.31 on 28 June, increasing to 1.34 on 9 July; but after July 9, with decay imminent, the ratio of an instantaneous to an average value obviously becomes an unacceptable comparison.

7 DISCUSSION AND CONCLUSIONS

7.1 The orbit determinations

The orbit has been determined daily from June 28 to July 11 and the sets of elements are given in Tables 1 and 2. In Table 2 three sets of elements for epochs July 10.0 and 11.0 are given, but the orbit C for both epochs is recommended because it was determined from observations spanning the epoch. The elements for orbit 15 (July 11.5) in Table 2 are converted from the orbital elements (orbit 14D) derived from the fitting of the observations between 08.08 and 16.02 UT on July 11.

The standard deviations of the orbital elements in the daily orbits from June 28.0 to July 11.0 correspond to radial and cross-track accuracies of 30 to 40 m. If these accuracies are realistic, the orbits are the most accurate ever published for such a high-drag satellite. Such a conclusion would not be too surprising, because the satellite was intensively observed by all the radars of the North American Air Defense Command, and also by the US Navy's Navspasur system and by several French radars, and all these observations were successfully used in the orbit determination. Furthermore the orbit refinement program used, Gooding's PROP 6, has proved itself to be extremely reliable for high-drag orbits, whenever the observations are confined to a time span of a day or two and the irregular variations in air drag are not too severe. Both these criteria are satisfied here, and there is no reason to suppose that errors of more than 20 m radial or

cross-track arise through errors in the PROP model. Despite these advantages, an accuracy of 30 to 40 m does seem somewhat over-optimistic, (a) because the observations have a basic accuracy of 100 to 200 m, and (b) because Skylab had a span of 27 m and a length of 26 m, and reflections could have come from different parts of the spacecraft. All in all, an accuracy of about 60 m radial and cross-track seems more realistic, and this is borne out by the analysis of inclination (section 3).

The fitting of the observations between 08.08 and 16.02 UT on July 11 - up to within 35 minutes of the burn-up - was remarkably good, and there seems no reason why the accuracy of this orbit (radial or cross-track) should be very much worse than the others. Degradation by a factor of about 2 might be expected and this is in conformity with the standard deviations obtained. So the orbit for noon on the last day should be accurate to about 100 m radial and cross-track, over the 8-hour time interval of the observations.

7.2 Other orbital work on Skylab 1

The decay of Skylab generated great interest because it was known that large pieces would survive decay, and these were seen as a threat to densely populated areas. NORAD/ NASA were issuing updated orbits at frequent intervals and these have been collected and presented by Wakker[25] from April 1978 until re-entry in July 1979. Carrou[26] records how the French covered the decay and gives plots of semi major axis and inclination from April to July 1979. However the main purpose of these determinations was to predict re-entry and not to analyse the orbital elements, and the cross-track accuracy achieved appears to be about 300 m.

The orbit of Skylab 1 was determined by Brookes and Moore[27] at 46 epochs between January 1974 and August 1976 using PROP 6 with 2100 observations from five sources; the Malvern Hewitt camera, the Cape kinetheodolite, the US Navy sensors, the Finnish theodolite and visual observers. Their orbits, which were used in determining air density, had average accuracies of 75 m and 130 m radial and cross-track respectively, but were of course at a time when drag was slight (M_2 averaged 0.01 deg/day^2, as compared with 1.6 to 60 deg/day^2 here).

7.3 The analysis of the orbits

The values of inclination have been analysed to obtain an average atmospheric rotation rate, Λ . The value found (Fig 6) was 1.10 ± 0.07 for an average height band of 210 to 220 km. This result, obtained after removing the resonance perturbations, conforms well with the results in Ref 12, where a value of 1.1 for Λ is indicated for average conditions. The values of inclination at 16th-order resonance have been successfully analysed (Fig 5), and lumped 16th-order geopotential coefficients $\bar{C}^{0,1}_{16}$ and $\bar{S}^{0,1}_{16}$ have been derived for the first time from resonance analysis. The values obtained were $10^9\bar{C}^{0,1}_{16} = 147 \pm 42$ and $10^9\bar{S}^{0,1}_{16} = 4 \pm 35$.

The air density has been determined at daily intervals at appropriate daily values of height. The density values have been standardized to a fixed value of exospheric temperature and are compared in Fig 8 with values of density derived from *CIRA 1972*. For the first 8 days the results indicate densities 15% lower than the annual-averaged *CIRA* values; however, the *CIRA* model gives a decrease of 14% in early

July due to the semi-annual variation. So it appears that the semi-annual variation in July 1979 conformed to that specified by the *CIRA 1972* model, in contrast to results from the early 1970s, when much larger semi-annual variations occurred[21].

The variation in eccentricity for Skylab has been analysed in detail and is found to follow that specified by the theory for an atmosphere with day-to-night variation in air density. In particular the observed increase in eccentricity a few days before decay (Fig 9) can be fully explained by the theory.

It has been shown that, in accordance with the theory for near-circular orbits about to decay in an atmosphere with day-to-night variation in density, the perigee moves towards the point of minimum density in the orbit. This process is illustrated in Fig 14. The combined movement of eccentricity and argument of perigee also conforms to theoretical expectations, as shown in Fig 13.

Acknowledgments

I wish to thank NORAD for supplying the observations on which this Report is based and Dr D.G. King-Hele for his helpful advice in the writing of this Report and for the analysis given in the Appendix.

Appendix

MEAN HEIGHT AT WHICH VALUES OF ρ OR Λ APPLY, WHEN DETERMINED FROM CIRCULAR ORBIT DECAY

If air density is determined from the decay rate of a circular orbit with radius that decreases from a_0 initially to a_1, at what value $\bar{a}$ of a does the density apply? To a first approximation, $\bar{a} \simeq \frac{1}{2}(a_0 + a_1)$, but a more accurate value is required here.

From equation (4.84) of Ref 18, the change $\Delta' a$ in one revolution due to drag in a spherically symmetrical atmosphere is

$$\Delta' a = -2\pi\delta a^2 \rho \quad , \tag{A-1}$$

where δ is the area/mass parameter and ρ is the air density at distance a from the Earth's centre, given by

$$\rho = \rho_0 \exp\left\{\beta(a_0 - a)\right\} \quad . \tag{A-2}$$

In equation (A-2), ρ_0 is the density at distance a_0 and $1/\beta = H$ is the density scale height. The rate of decrease of a at any time, da/dt, is $\Delta' a/T$, where T is the orbital period, equal to $2\pi/n$, where n is the mean motion. Thus, from (A-1),

$$\frac{da}{dt} = -n\delta a^2 \rho \quad , \tag{A-3}$$

whence

$$\exp\left\{\beta(a - a_0)\right\}\frac{da}{dt} = -n\delta a^2 \rho_0 \tag{A-4}$$

from (A-2). Since na^2 does not vary by more than 0.2% in one day for 1973-27A, we may take

$$n\delta a^2 \rho_0 = k \tag{A-5}$$

as constant, so that (A-4) may be integrated between $t = t_0$ and $t = t_1$ to give

$$1 - \exp\left\{\beta(a_1 - a_0)\right\} = \beta k(t_1 - t_0) \quad . \tag{A-6}$$

Since the rate of change of a is proportional to ρ by (A-3), the mean density $\bar{\rho}$ between times t_0 and t_1 is given by

$$\bar{\rho} = \frac{1}{t_1 - t_0}\int_{t_0}^{t_1} \rho dt = -\frac{1}{t_1 - t_0}\int_{a_0}^{a_1} \frac{da}{n\delta a^2} \quad , \tag{A-7}$$

on using (A-3). From (A-7) and (A-5),

$$\frac{\bar{\rho}}{\rho_0} = \frac{1}{k(t_1 - t_0)}\int_{a_1}^{a_0} da = \frac{a_0 - a_1}{k(t_1 - t_0)} \quad . \tag{A-8}$$

On using (A-2) and (A-6), equation (A-8) becomes

$$\exp\left\{\beta(a_0 - \bar{a})\right\} = \frac{\beta(a_0 - a_1)}{1 - \exp\left\{\beta(a_1 - a_0)\right\}}$$

which gives

$$a_0 - \bar{a} = H \ln\left[\frac{\beta(a_0 - a_1)}{1 - \exp\left\{-\beta(a_0 - a_1)\right\}}\right] . \qquad \text{(A-9)}$$

If $\beta(a_0 - a_1)$ is small, equation (A-9) can be expanded in powers of $\beta(a_0 - a_1)$ to give

$$\frac{a_0 - \bar{a}}{a_0 - a_1} = \frac{1}{2} - \frac{\beta(a_0 - a_1)}{24} + O\left[\frac{\left\{\beta(a_0 - a_1)\right\}^3}{60}\right] . \qquad \text{(A-10)}$$

For 1973-27A, equation (A-10) is adequate except for the last day, when $\beta(a_0 - a_1) = 0.82$ and (A-9) is needed.

The effects of atmospheric oblateness introduce a factor $(1 + \frac{1}{2}c^2)$ into the right-hand side of equation (A-1), as shown by equation (5.49) of Ref 18. Since this differs from 1 only by second-order terms, and is constant, the analysis should also be valid for an oblate atmosphere.

Since the change in inclination Δi is proportional to ρ, the same analysis should be valid, and the values of rotation rate Λ obtained by fitting the decrease in inclination may be taken as applying at the distance $\bar{a}$ given by (A-9).

REFERENCES

No.	Author	Title, etc
1	D.G. King-Hele J.A. Pilkington H. Hiller D.M.C. Walker	*The RAE table of Earth satellites 1957-1980.* Macmillan Press, London (1981)
2	L.F. Belew	*Skylab, our first space station.* NASA SP-400, Washington (1977)
3	J.A. Pilkington D.G. King-Hele H. Hiller	Table of Earth satellites, Volume 2 : 1969-1973 RAE Technical Report 74105 (1974)
4	A. Wilson	Skylab - the last hours. *Spaceflight*, 22, No.1, 36-37 (1980)
5	R.H. Gooding	The evolution of the PROP 6 orbit determination program, and related topics. RAE Technical Report 74164 (1974)
6	P.E. Dreher R.P. Little G. Wittenstein	Skylab orbital lifetime prediction and decay analysis. NASA Technical Memorandum 78308 (1980)
7	G.E. Cook	PROD, a computer program for predicting the development of drag-free satellites. Part 1: theory. RAE Technical Report 71007 (1971) [*Celestial Mechanics*, 7, 301-314 (1973)]
8	T.L. Felsentreger J.G. Marsh R.W. Agreen	Analysis of the solid earth and ocean tidal perturbations on the orbits of the Geos 1 and Geos 2 satellites. *Journ. Geophys. Res.*, 81, 2557-2563 (1976)
9	J.W. Slowey	Systematic winds at heights between 350 and 675 km from analysis of the orbits of four balloon satellites. *Planet. Space Sci.*, 23, 879-886 (1975)
10	D.M.C. Walker	Cosmos 462 (1971-106A): orbit determination and analysis. *Phil. Trans. Roy. Soc. A*, 292, 473-512 (1979) RAE Technical Report 78089 (1978)
11	D.G. King-Hele	The effect of a meridional wind on a satellite orbit. *Proc. Roy. Soc. A*, 294, 261-272 (1966) RAE Technical Report 66010 (1966)
12	D.G. King-Hele D.M.C. Walker	Upper-atmosphere zonal winds: variation with height and local time. *Planet. Space Sci.*, 25, 313-336 (1977) RAE Technical Report 76055 (1976)
13	R.H. Gooding	Lumped geopotential coefficients $\bar{C}_{15,15}$ and $\bar{S}_{15,15}$ obtained from resonant variation in the orbit of Ariel 3. RAE Technical Report 71068 (1971)

REFERENCES (continued)

No.	Author	Title, etc
14	H. Hiller	Upper-atmosphere rotation rate determined from the orbit of China 6 rocket (1976-87B). *Planet. Space Sci.*, 28, 549-558 (1980) RAE Technical Report 79115 (1979)
15	D.G. King-Hele	Skylab 1 rocket, 1973-27B: orbit determination and analysis. *Phil. Trans. Roy. Soc. A*, 296, 597-637 (1980) RAE Technical Report 79044 (1979)
16	F.J. Lerch B.H. Putney C.A. Wagner S.M. Klosko	Goddard Earth Models for oceanographic applications (GEM 10B and 10C). *Marine Geodesy*, 5(2), 145-187 (1981)
17	D.M.C. Walker	Analysis of the US Navy orbits of 1963-24B and 1974-34A at 15th-order resonance. *Geophys. J.R. Astr. Soc.*, 67, 1-18 (1981) RAE Technical Report 80093 (1980)
18	D.G. King-Hele	*Theory of satellite orbits in an atmosphere.* Butterworths, London (1964)
19	G.E. Cook D.G. King-Hele	The contraction of satellite orbits under the influence of air drag, Part VI. Near-circular orbits with day-to-night variation in air density. *Proc. Roy. Soc. A*, 303, 17-35 (1968) RAE Technical Report 67092 (1967)
20	-	*CIRA 1972* (COSPAR International Reference Atmosphere 1972). Akademie-Verlag, Berlin (1972)
21	D.M.C. Walker	Variations in air density from January 1972 to April 1975 at heights near 200 km. *Planet. Space Sci.*, 26, 291-309 (1978) RAE Technical Report 77078 (1977)
22	A. Eisner S.M. Yionoulis	Neutral density variations in the 900-1200 km region of the upper atmosphere. *Ann. Géophys., t. 37, fasc. 1,* 235-240 (1981)
23	L.G. Jacchia	Thermospheric temperature, density, and composition : new models. Smithsonian Astrophysical Observatory Special Report 375 (1977)
24	G.E. Cook D.G. King-Hele	The contraction of satellite orbits under the influence of air drag, Part V. With day-to-night variation in air density. *Phil. Trans. Roy. Soc., A*, 259, 33-67 (1965) RAE Technical Report 64029 (1964)

REFERENCES (concluded)

No.	Author	Title, etc
25	K.F. Wakker	De standregeling en de baan van Skylab gedurende de periode April 1978 tot Juli 1979. Technische Hogeschool Delft, Rapport LR-288 (1979)
26	J.P. Carrou	Skylab decay follow-up. *Spacecraft flight dynamics*, proceedings of an international symposium, ESA SP-160, 421-430 (1981)
27	C.J. Brookes P. Moore	Air density at heights near 435 km from the orbit of Skylab 1 (1973-27A). *Planet. Space Sci.*, 26, 913-924 (1978)

Fig 1

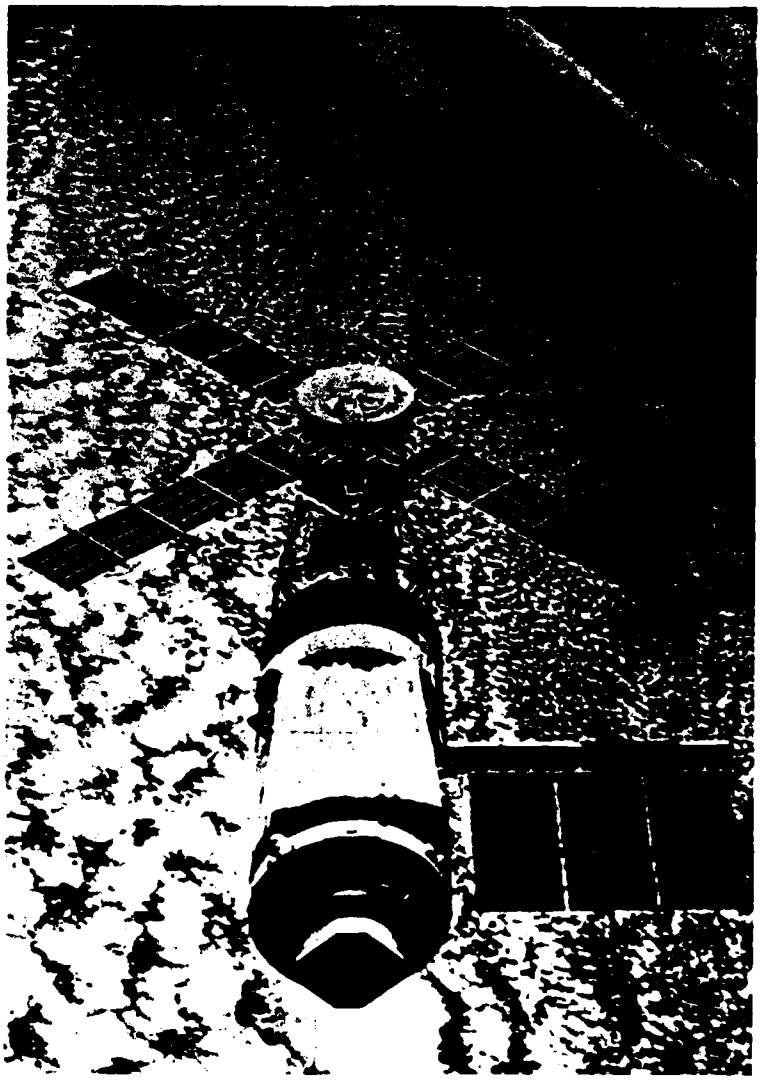

Fig 1 Skylab 1 in flight

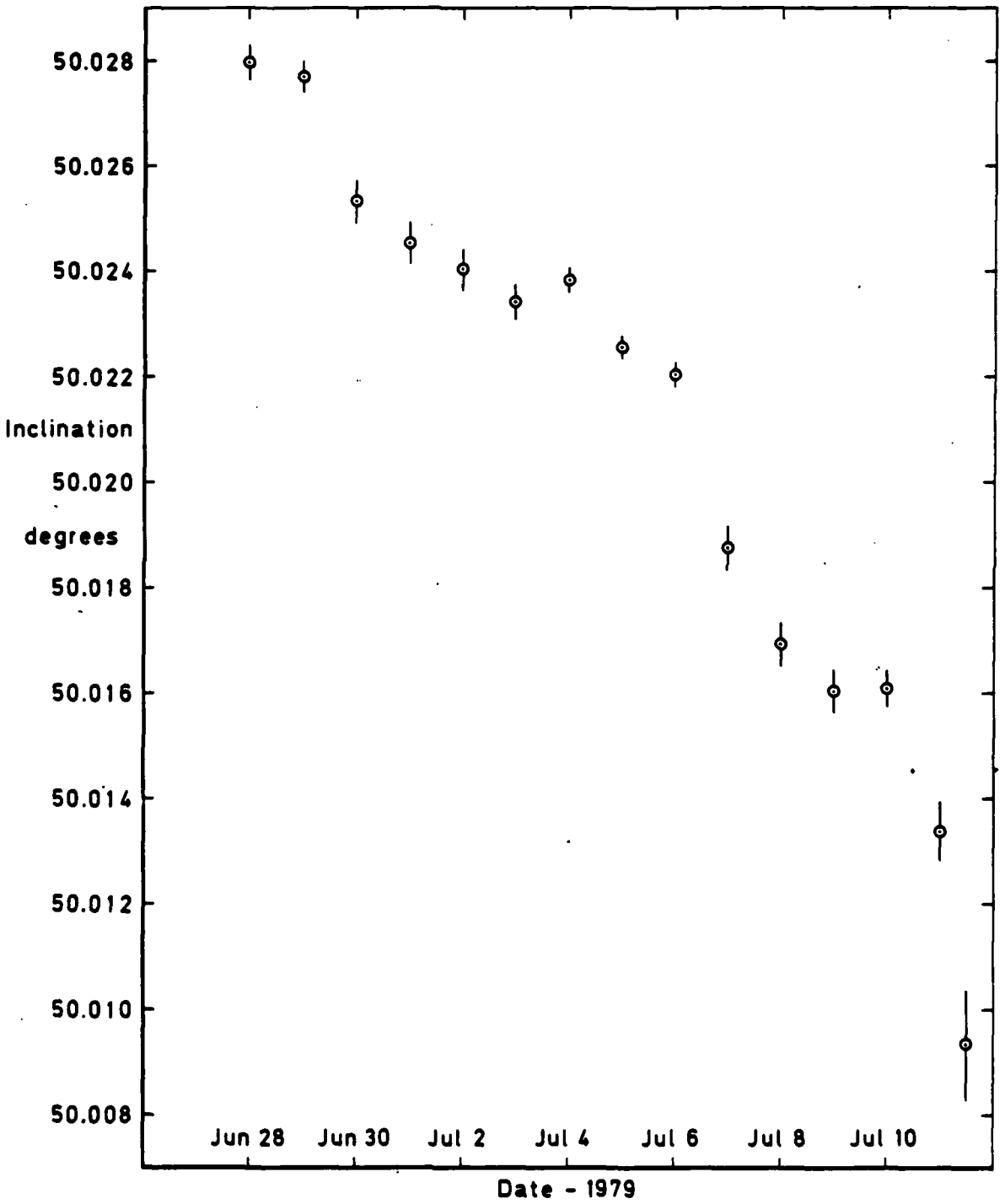

Fig 2 Values of inclination from Tables 1 and 2

Fig 3

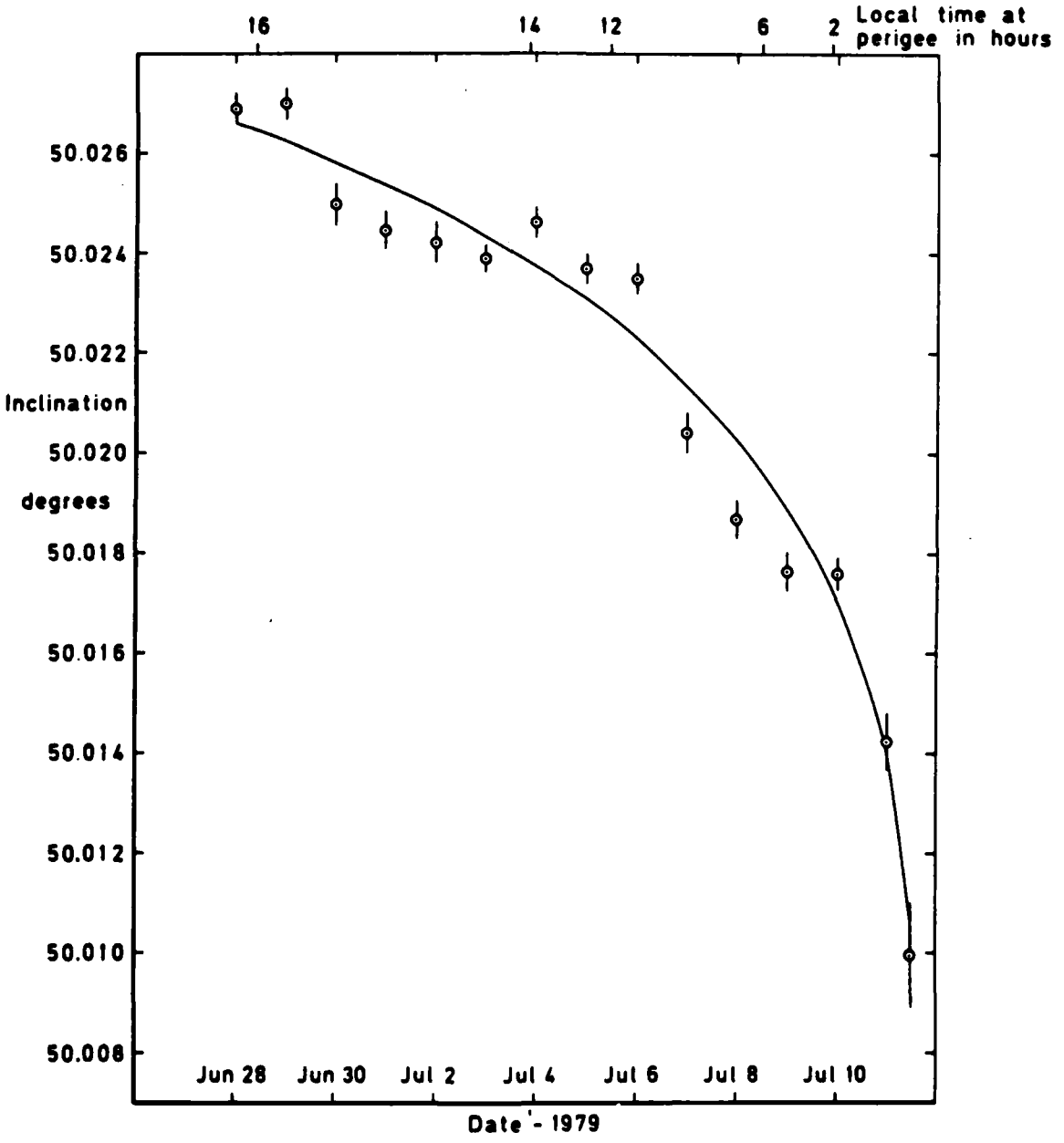

Fig 3 Values of inclination, cleared of zonal harmonic, $J_{2,2}$ and lunisolar perturbations, with fitted curve for $\Lambda = 1.25$

TR 82067

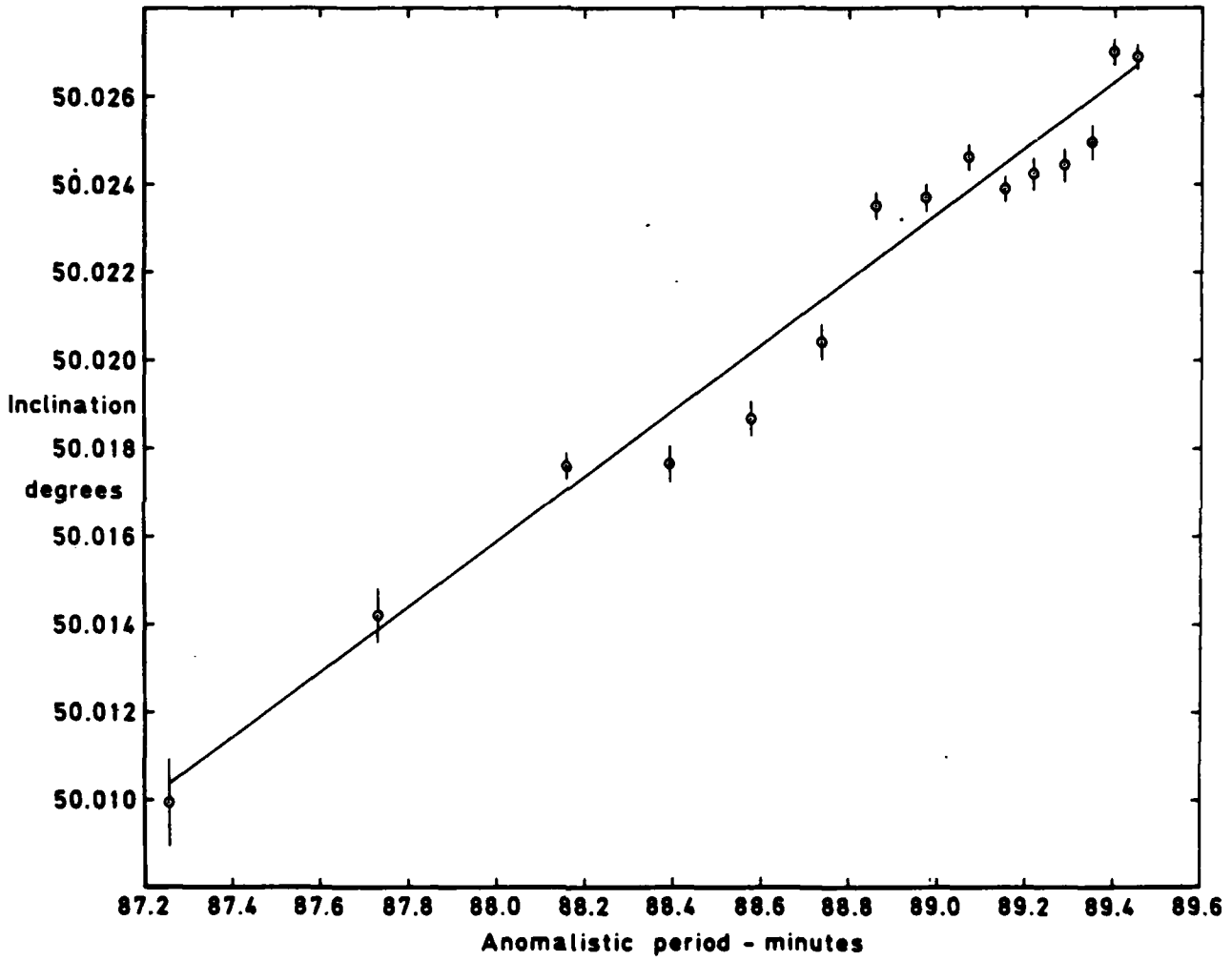

Fig 4 Values of inclination from Fig 3 plotted against period, with fitted straight line

Fig 5

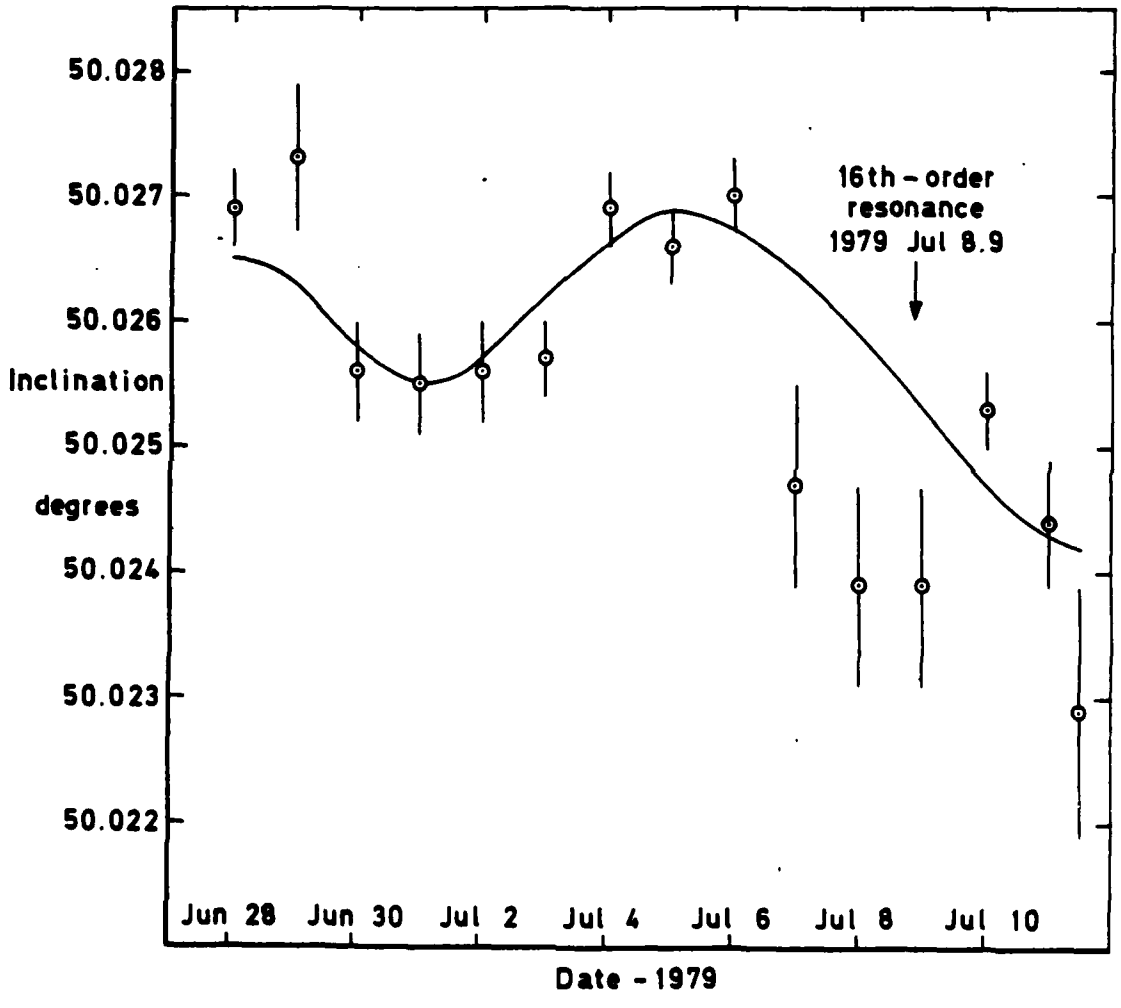

Fig 5 Values of inclination, cleared of zonal harmonic, $J_{2,2}$ and lunisolar perturbations, with fitted curve for 16th-order resonance

TR 82067

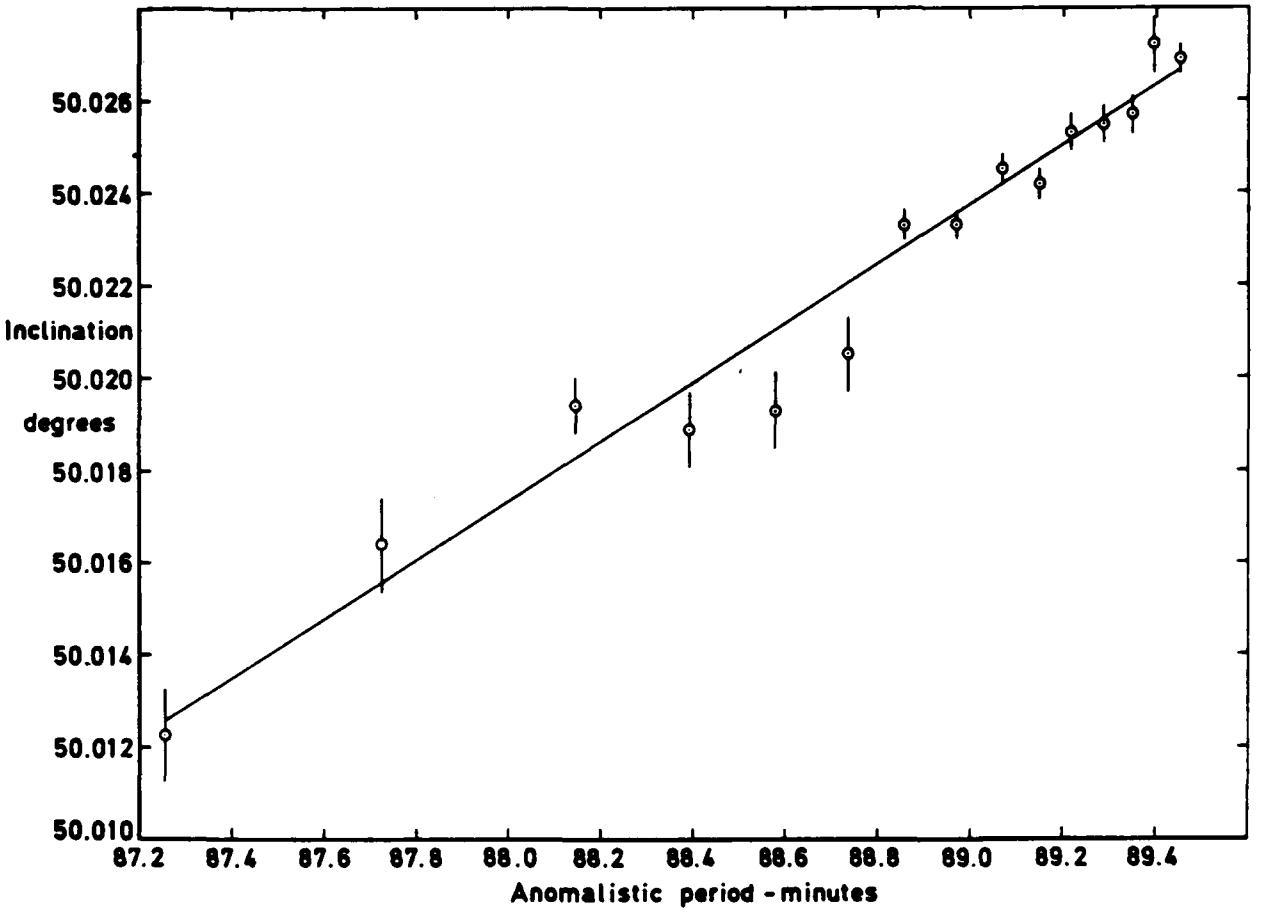

Fig 6 Values of inclination, cleared of zonal harmonic, $J_{2,2}$, lunisolar and resonance perturbations, with fitted curve

Fig 7

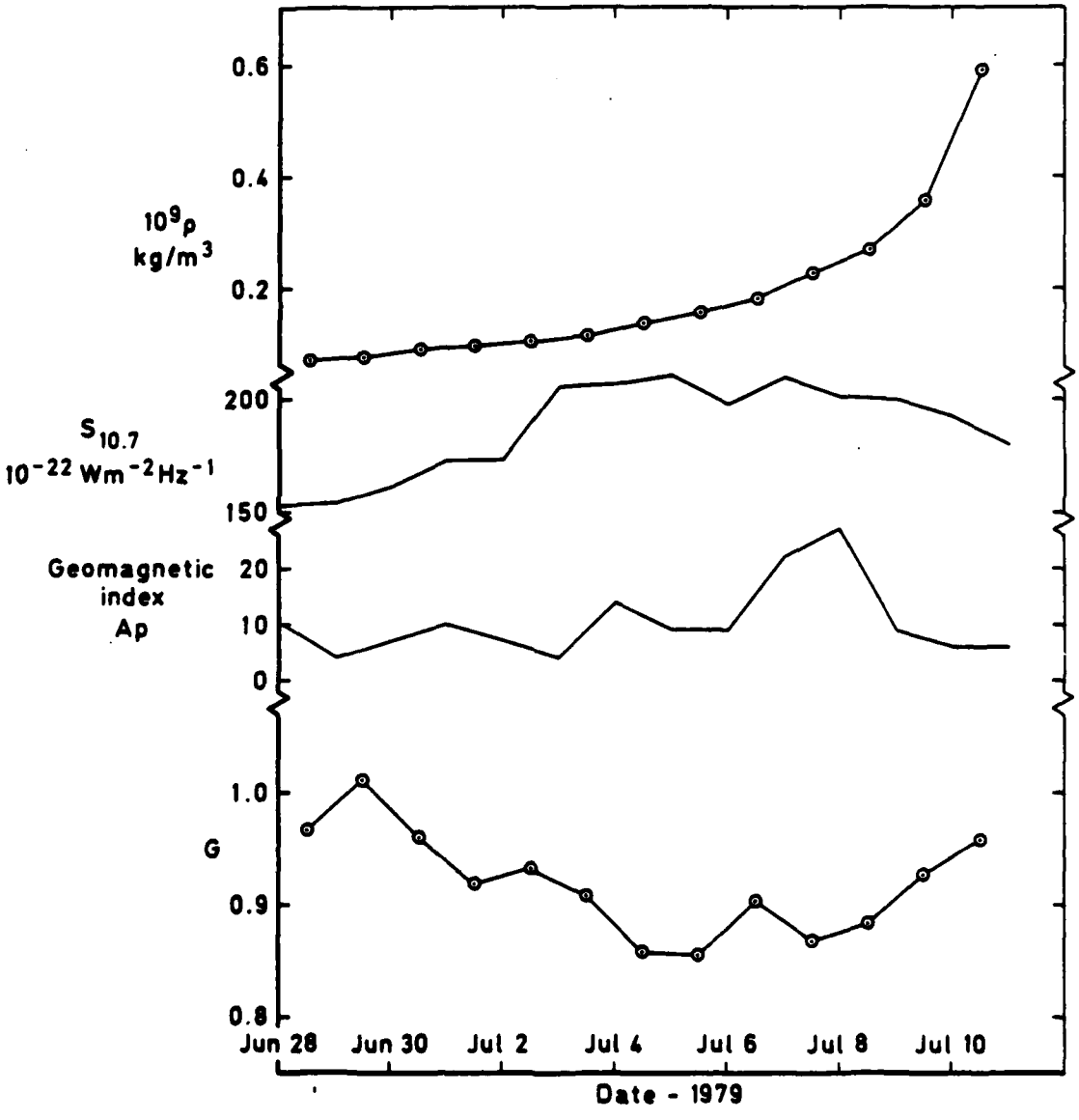

Fig 7 Values of density ρ and density ratio G, with solar radiation energy $S_{10.7}$ and geomagnetic index Ap

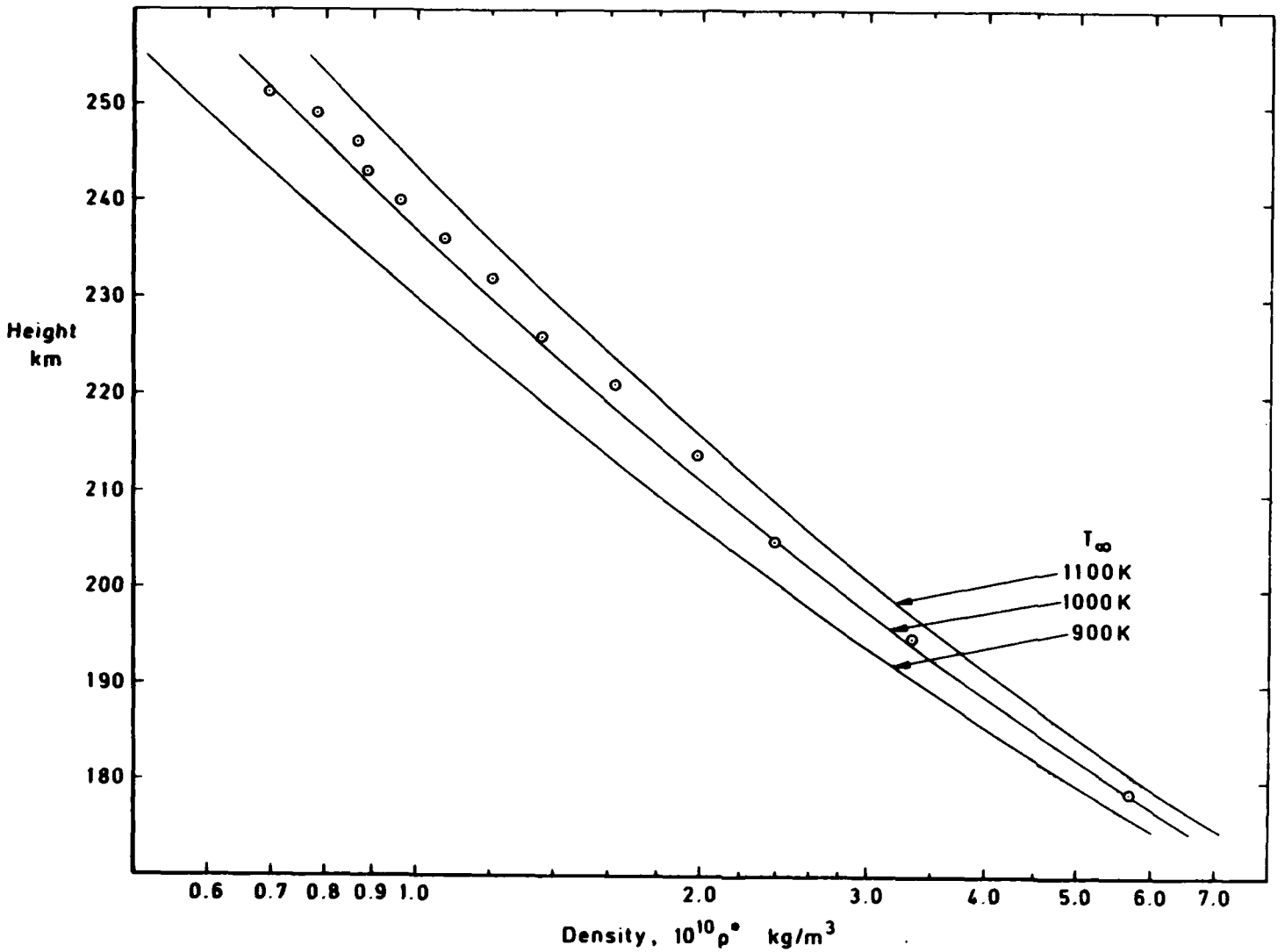

Fig 8 Values of density ρ^*, with curves from CIRA 1972 for exospheric temperatures 900–1100K

Fig 8

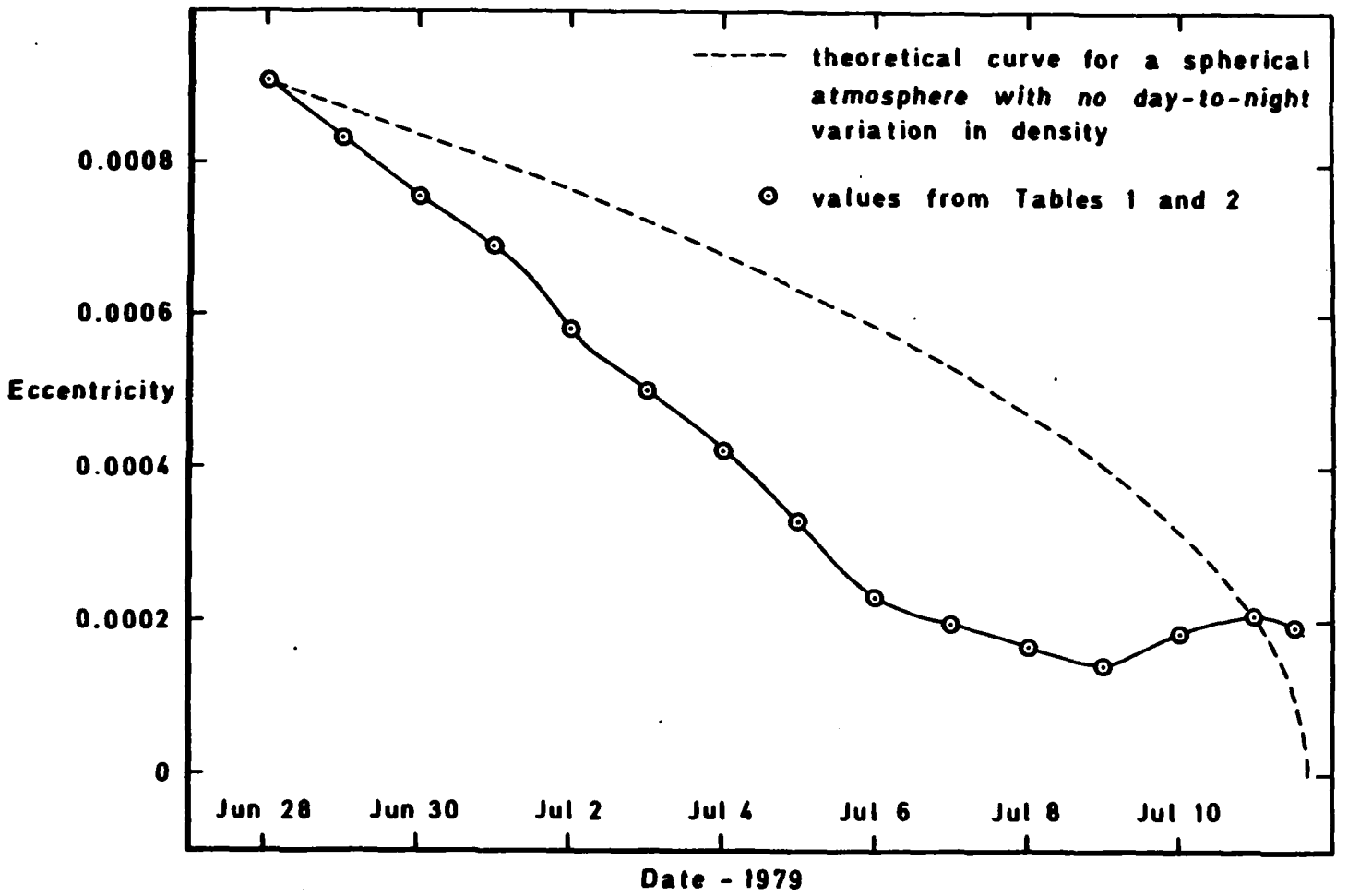

Fig 9 Values of eccentricity from Tables 1 and 2

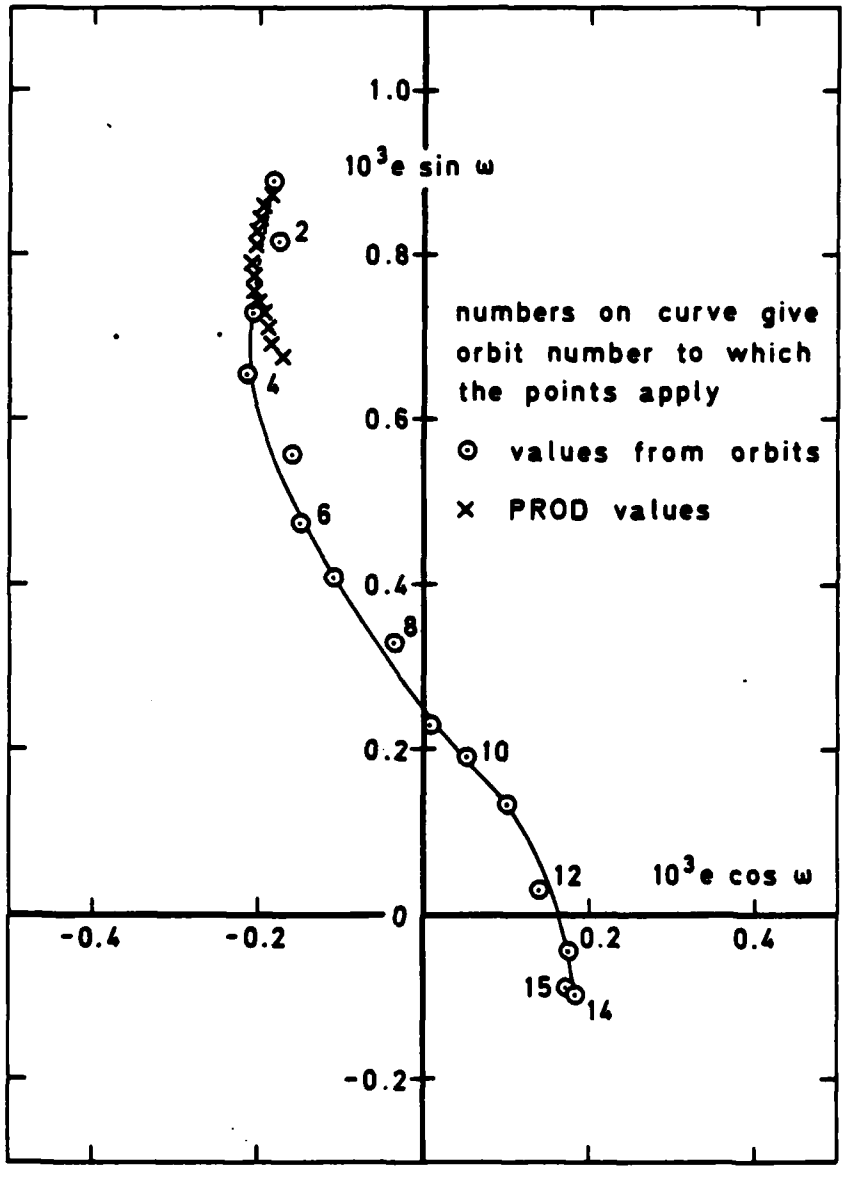

TR 82067

Fig 10 Values of e sin ω and e cos ω from the 15 orbits (circles) and the zero-drag PROD values (crosses)

Fig 11

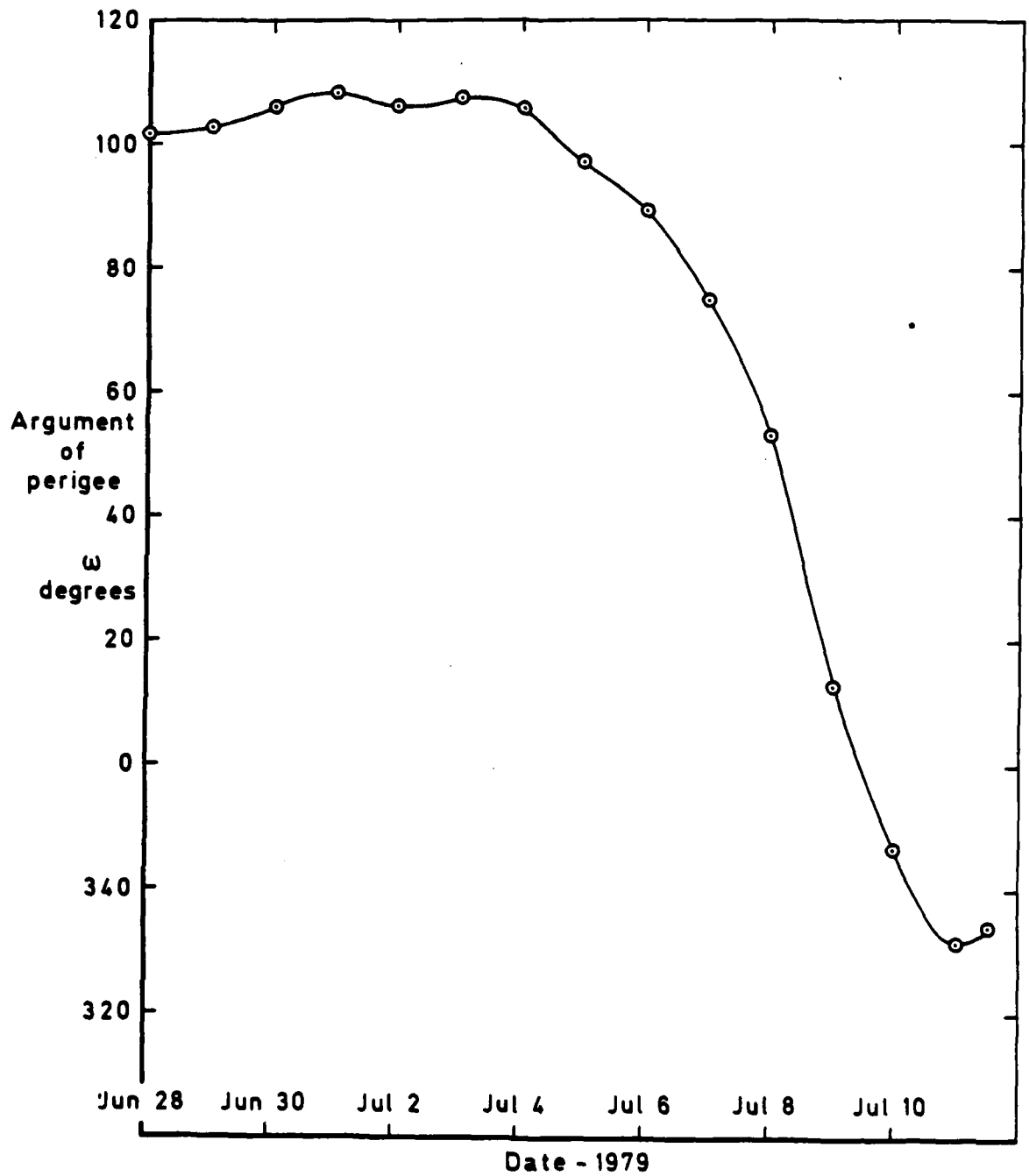

Fig 11 Values of argument of perigee, ω, from Tables 1 and 2

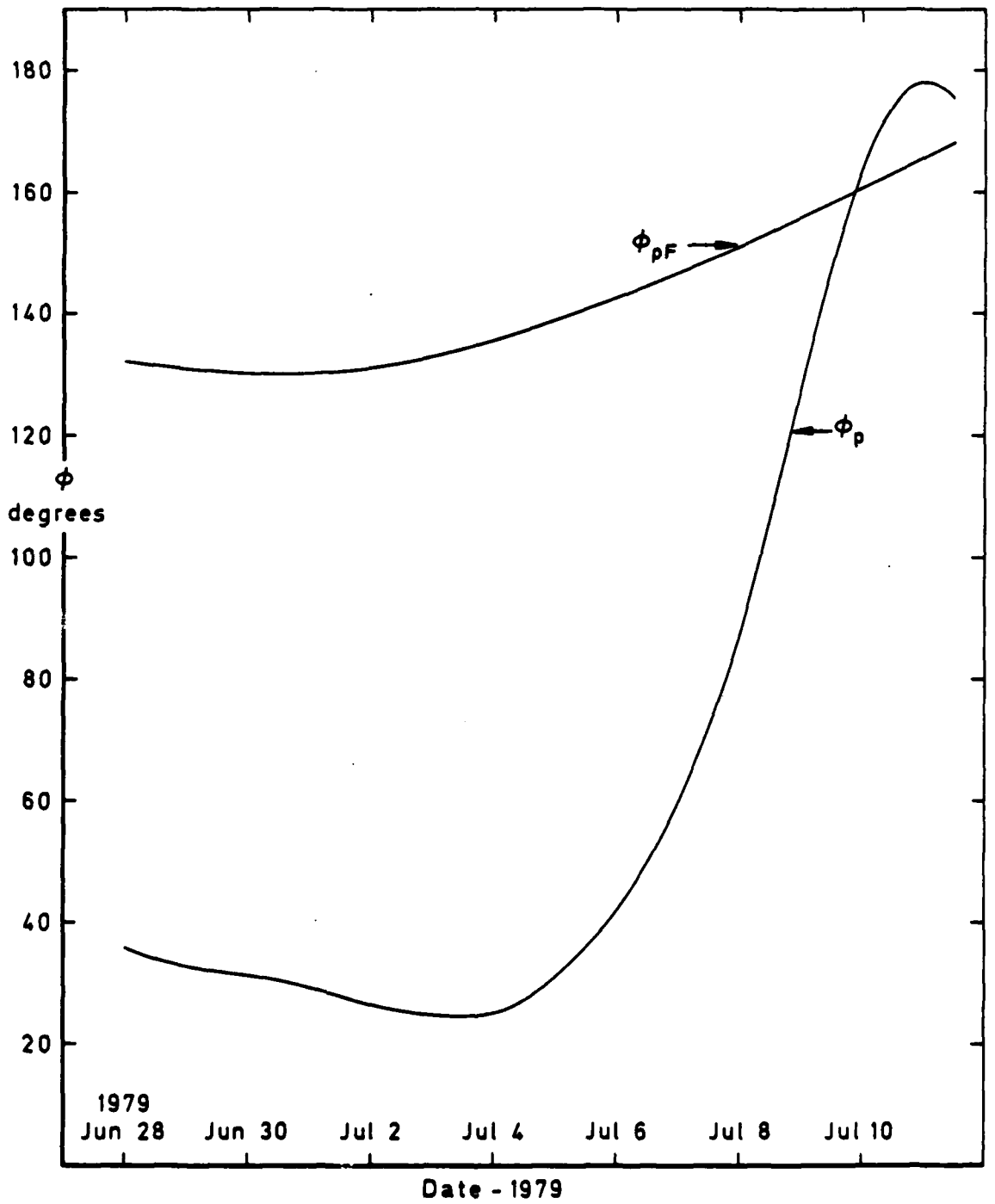

Fig 12 Values of ϕ_p, the bulge-perigee angle, and ϕ_{pF}, given by equation (10)

Fig 13

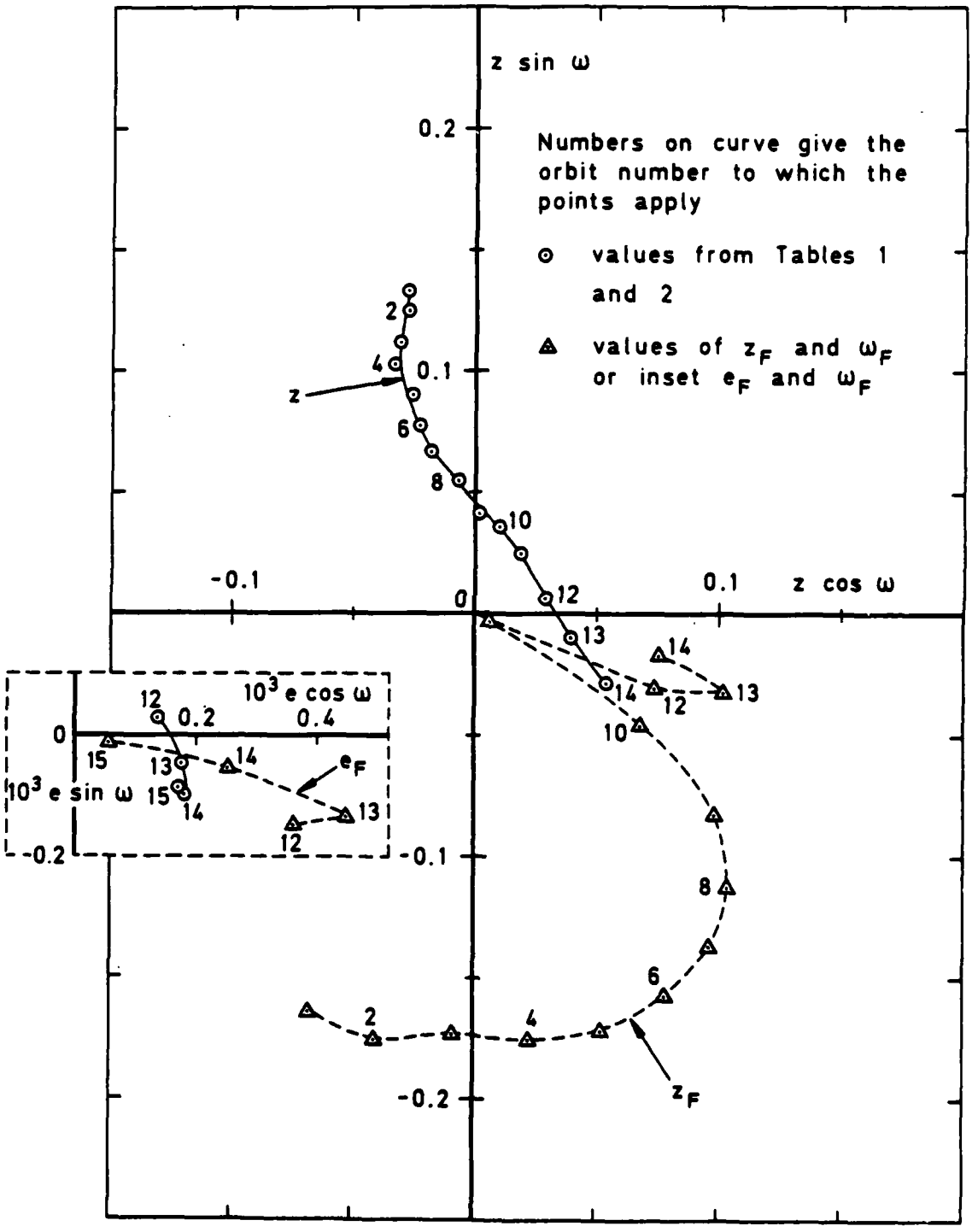

Fig 13 Values of z and ω, z_F and ω_F and, inset, e and e_F

(a) Notation

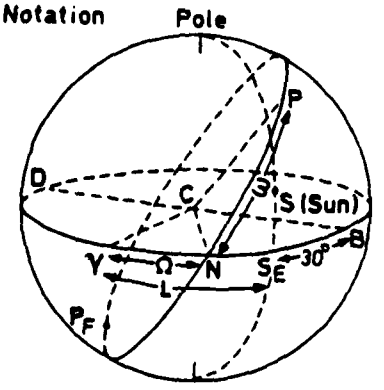

B	Maximum density point
C	Earth's centre
D	Minimum density point
L	Longitude of the Sun
M′	Angle BCN $(\Omega-L-30)^\circ$
N	Ascending node of satellite
P	Perigee position
P_F	Point of minimum density in the orbital plane
S	Sun's position
S_E	Equatorial Sun
Υ	First point of Aries
ω	Argument of perigee
Ω	Longitude of ascending node

(b) Orbit 1

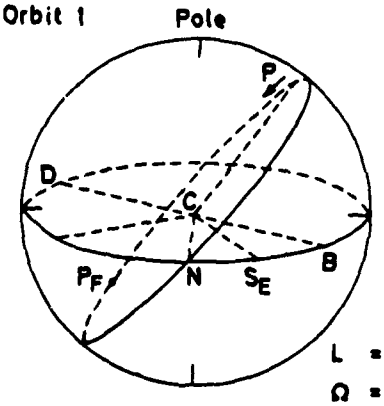

$L = 96^\circ$
$\Omega = 51^\circ$
$\omega = 102^\circ$
$\omega_F = 247^\circ$

(c) Orbit 4

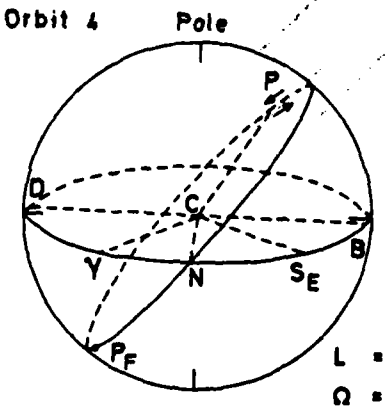

$L = 99^\circ$
$\Omega = 34^\circ$
$\omega = 108^\circ$
$\omega_F = 277^\circ$

(d) Orbit 10

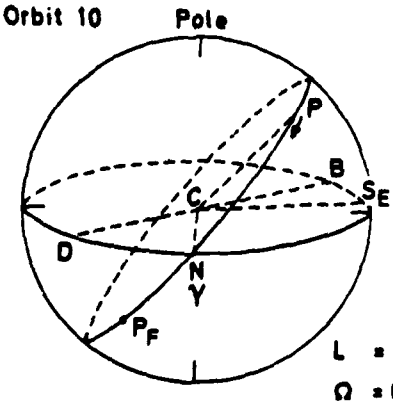

$L = 104^\circ$
$\Omega = 0$
$\omega = 75^\circ$
$\omega_F = 327^\circ$

(e) Orbit 14

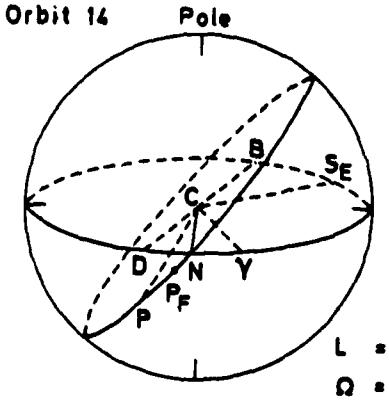

$L = 108^\circ$
$\Omega = 337^\circ$
$\omega = 332^\circ$
$\omega_F = 348^\circ$

Fig 14a-e Sketches showing the progress of the perigee point P towards the point of minimum density P_F in the orbital plane

Fig 15

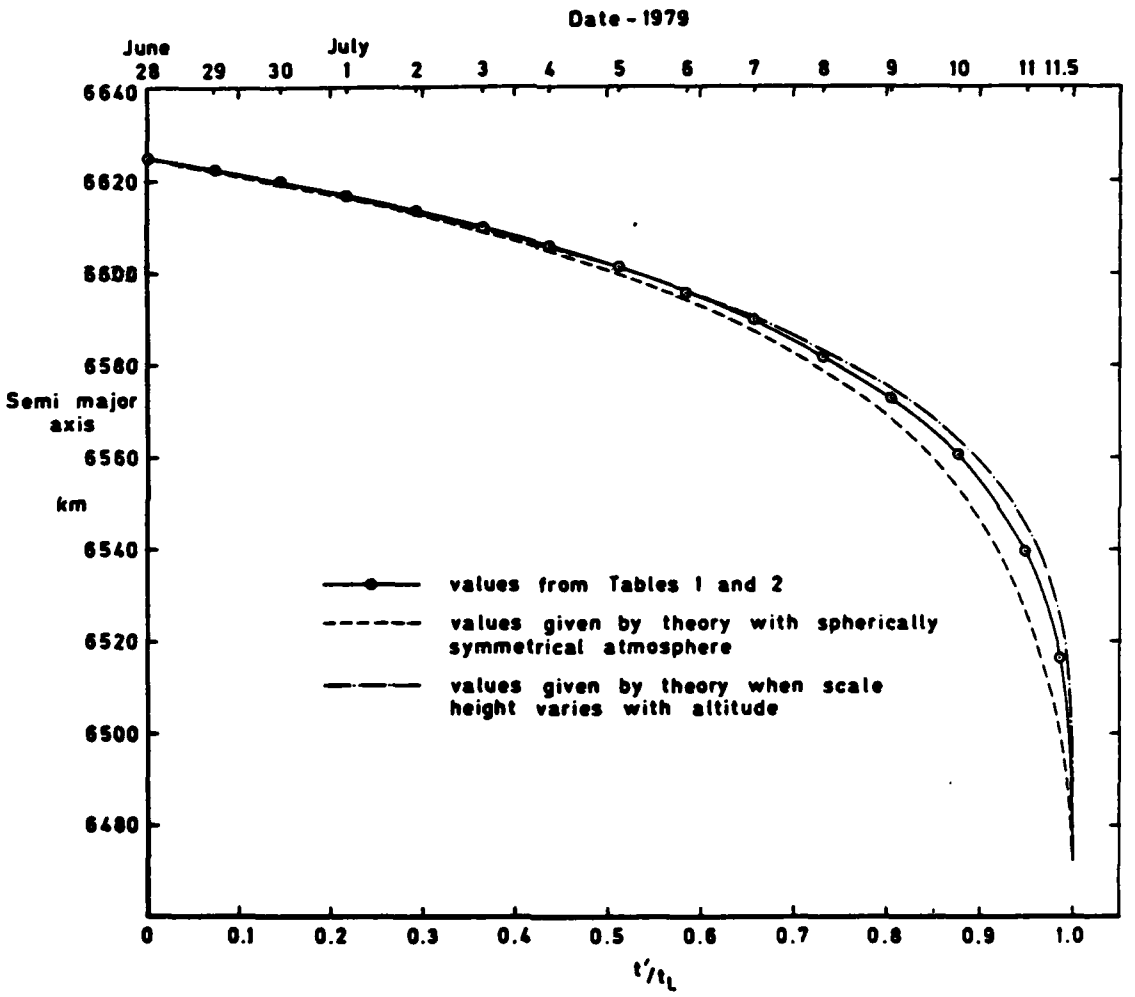

Fig 15 Values of semi major axis from Tables 1 and 2, with theoretical curves

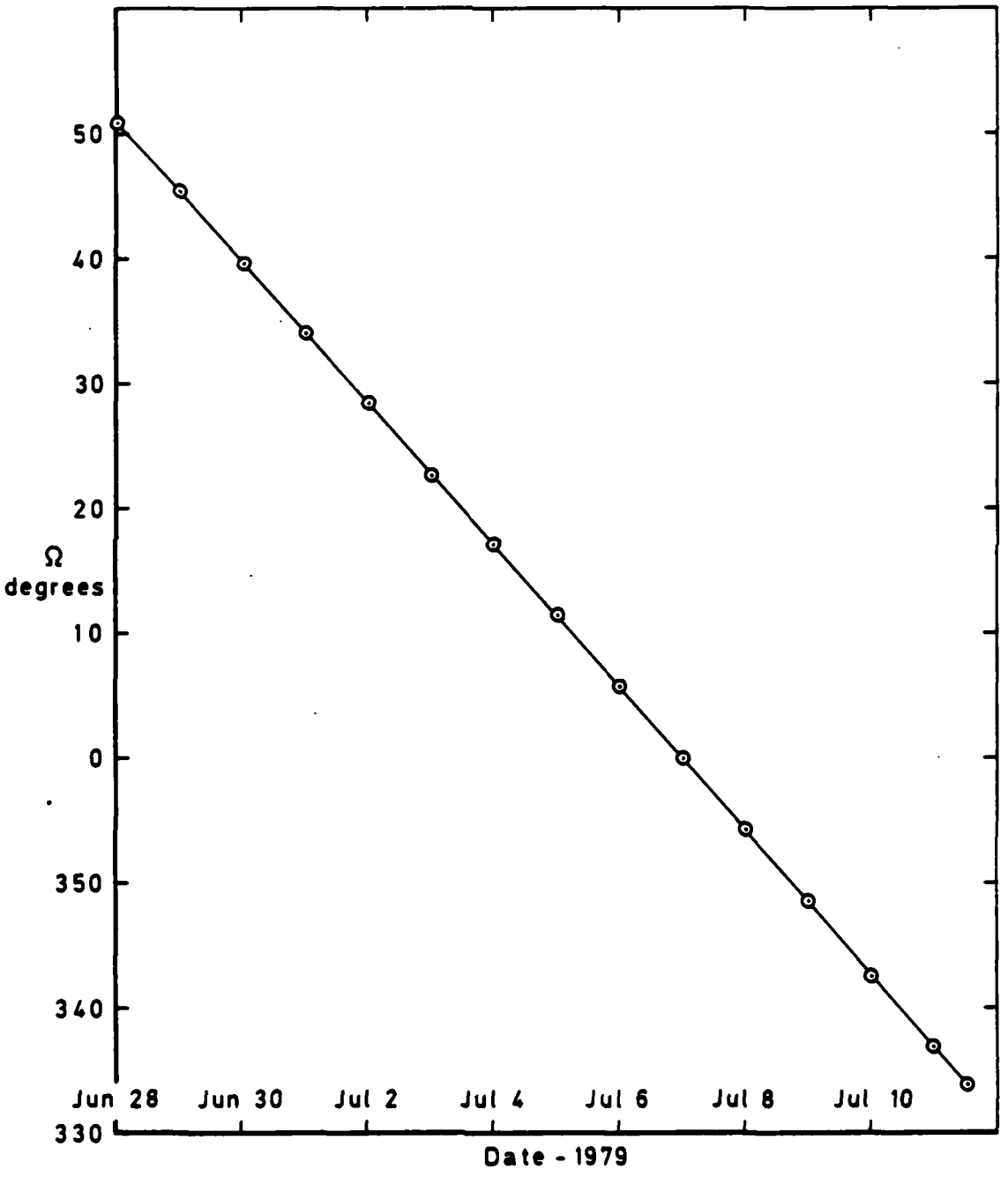

Fig 16 Values of Ω from Tables 1 and 2

Fig 17

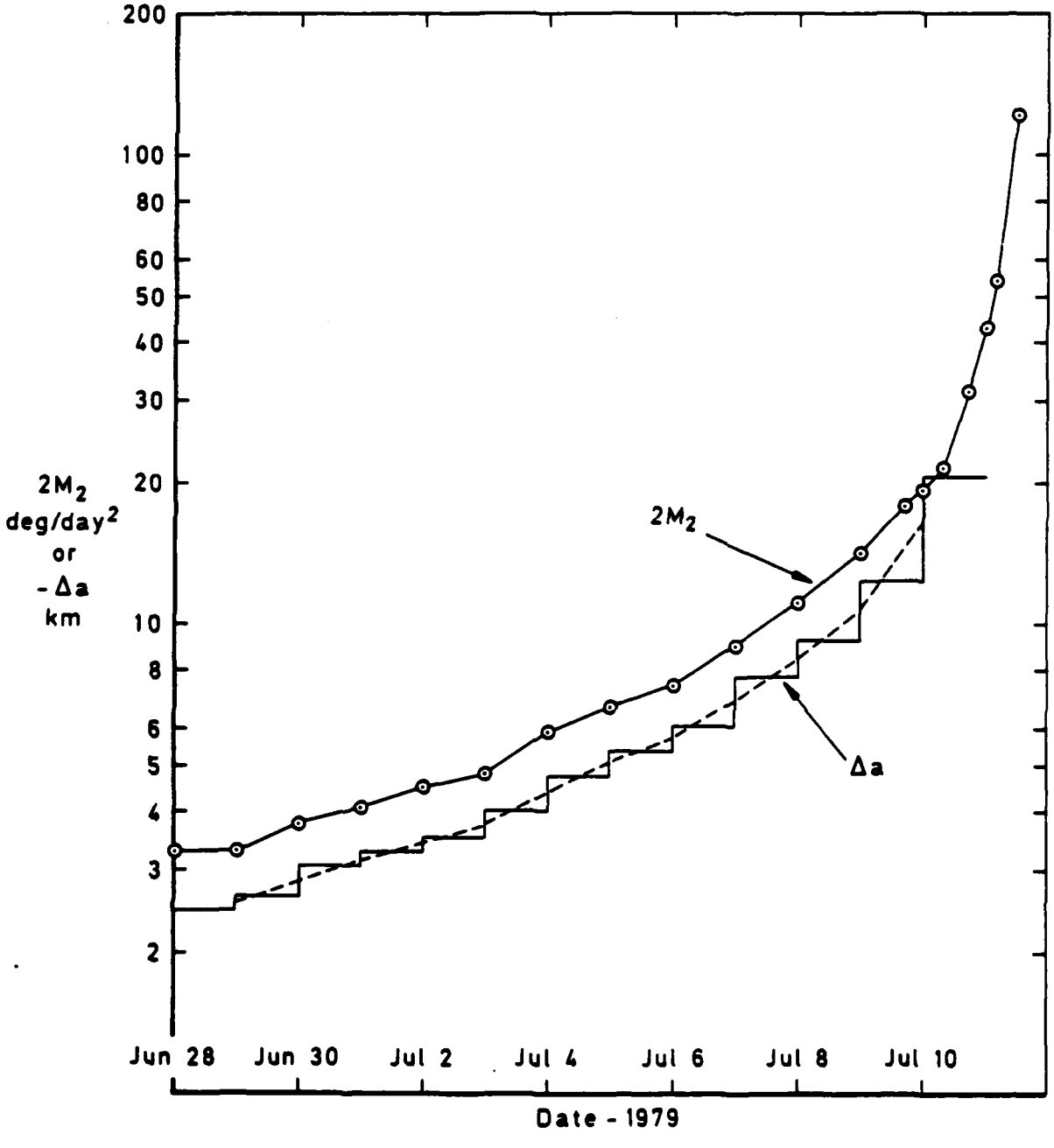

Fig 17 Values of $2M_2$ and Δa (the daily change in a)

TR 82067

REPORT DOCUMENTATION PAGE

Overall security classification of this page

~~UNCLASSIFIED~~ UNLIMITED

As far as possible this page should contain only unclassified information. If it is necessary to enter classified information, the box above must be marked to indicate the classification, e.g. Restricted, Confidential or Secret.

1. DRIC Reference (to be added by DRIC)	2. Originator's Reference	3. Agency Reference	4. Report Security Classification/Marking
	RAE TR 82067	N/A	~~UNCLASSIFIED~~ UNLIMITED

5. DRIC Code for Originator	6. Originator (Corporate Author) Name and Location
7673000W	Royal Aircraft Establishment, Farnborough, Hants, UK

5a. Sponsoring Agency's Code	6a. Sponsoring Agency (Contract Authority) Name and Location
N/A	N/A

7. Title

The last 14 days of Skylab 1: orbit determination and analysis

7a. (For Translations) Title in Foreign Language

7b. (For Conference Papers) Title, Place and Date of Conference

8. Author 1. Surname, Initials	9a. Author 2	9b. Authors 3, 4	10. Date	Pages	Refs.
Walker, Doreen M.C.			June 1982	43	27

11. Contract Number	12. Period	13. Project	14. Other Reference Nos.
N/A	N/A		Space 617

15. Distribution statement

(a) Controlled by –

(b) Special limitations (if any) –

16. Descriptors (Keywords) (Descriptors marked * are selected from TEST)

Skylab. Orbits. Orbital theory. Upper atmosphere density and winds. Resonance.

17. Abstract

The orbit of Skylab 1 (1973-27A) has been determined using some 1400 NORAD observations during the 14 days prior to decay on 1979 July 11. There are 14 daily orbits, with standard deviations corresponding to average accuracies of 40 m cross track and 30 m radial. A 15th orbit, only slightly less accurate, was determined from observations on July 11 between the manoeuvre at 07.45 UT and decay at 16.37 UT.

The variations in inclination due to atmospheric rotation and 16th-order resonance with the geopotential have been successfully analysed, to give the first values of 16th-order geopotential coefficients determined from resonance, and a value of 1.10 ± 0.07 rev/day for the atmospheric rotation rate at a height of 210-220 km.

The daily changes in semi-major axis have been used to determine 13 daily values of air density, at heights from 252 km down to 179 km. All agree well with the *CIRA 1972* model, and indicate a smaller semi-annual variation than in the early 1970s.

The variations of eccentricity and argument of perigee take unusual forms, but detailed analysis shows that the variations are in full accord with the theory for an atmosphere with day-to-night variation in density, with the perigee progressing